



Tom Ducat

The 3-dimensional Lyness map and a self-mirror log Calabi–Yau 3-fold

Received: 29 October 2021 / Accepted: 30 June 2023 / Published online: 3 August 2023

Abstract. The 2-dimensional Lyness map is a 5-periodic birational map of the plane which may famously be resolved to give an automorphism of a log Calabi–Yau surface, given by the complement of an anticanonical pentagon of (-1) -curves in a del Pezzo surface of degree 5. This surface has many remarkable properties and, in particular, it is mirror to itself. We construct the 3-dimensional big brother of this surface by considering the 3-dimensional Lyness map, which is an 8-periodic birational map. The variety we obtain is a special (non- \mathbb{Q} -factorial) affine Fano 3-fold of type V_{12} , and we show that it is a self-mirror log Calabi–Yau 3-fold.

Contents

1. Introduction	87
2. Mirror symmetry and log Calabi–Yau varieties	91
3. Dimension 2: the del Pezzo surface dP_5	104
4. Dimension 3: the Fano 3-fold V_{12}	114
References	139

1. Introduction

1.1. The Lyness map

Definition 1.1. The d -dimensional Lyness map $\sigma_d \in \text{Bir}(\mathbb{C}^d)$ is the birational map

$$\sigma_d(x_1, x_2, \dots, x_{d-1}, x_d) = \left(x_2, x_3, \dots, x_d, \frac{1 + x_2 + \dots + x_d}{x_1} \right).$$

By iterating $\sigma_d^{\pm 1}$, we can consider an associated sequence of rational functions $(x_i : i \in \mathbb{Z})$, where $x_i \in \mathbb{C}(x_1, \dots, x_d)$ is defined inductively for $i > d$ and $i < 1$ by using the d -dimensional Lyness recurrence relation

$$x_i x_{d+i} = 1 + x_{i+1} + \dots + x_{d+i-1}, \quad \forall i \in \mathbb{Z}. \tag{LR_d}$$

T. Ducat (✉) Durham University, Durham, UK
 e-mail: thomas.ducat@durham.ac.uk

Mathematics Subject Classification: 14J33

Low dimensional behaviour In dimensions $d \leq 3$ the recurrence relation (LR_d) is very well behaved, with two very nice and surprising properties: it is *periodic*, and the sequence of rational functions $(x_i : i \in \mathbb{Z})$ possesses a *Laurent phenomenon*. In other words, this sequence is actually a sequence of Laurent polynomials $x_i \in \mathbb{C}[x_1^{\pm 1}, \dots, x_d^{\pm 1}]$.

Higher dimensional behaviour Unfortunately, for all $d \geq 4$ the recurrence relation (LR_d) is much more badly behaved, something that is also reflected in the dynamical behaviour of σ_d . It is no longer periodic; nor does it have a Laurent phenomenon. Because of this there seems to be no straightforward way of generalising the very attractive log Calabi–Yau varieties (or their scattering diagrams) described in this paper when $d = 2$ or 3 .

1.2. A tale of two log Calabi–Yau varieties

The two recurrences (LR_2) and (LR_3) can be used to construct two affine log Calabi–Yau varieties. The first is the famous affine del Pezzo surface of degree 5; the second is an affine Fano 3-fold of type V_{12} .¹ As we will recall in Sect. 2, affine log Calabi–Yau varieties (satisfying some suitable technical hypotheses) are expected to enjoy some remarkable properties coming from mirror symmetry. In particular, there is a conjectural involution on the set of such varieties which, for a given log Calabi–Yau variety U , associates a *mirror* U^* . According to a conjecture of Gross, Hacking & Keel (cf. Conjecture 2.5), one feature of the relationship between U and U^* is that there is expected to be a special additive basis of the coordinate ring of U^* , called the basis of *theta functions*, whose elements correspond (roughly speaking) to boundary divisors in compactifications of U , and vice-versa.

1.2.1. Dimension 2 and the del Pezzo surface dP_5 In dimension 2 the recurrence relation (LR_2) generates a 5-periodic sequence $(x_i : i \in \mathbb{Z}/5\mathbb{Z})$. In terms of x_1 and x_2 , the solution is given by

$$x_3 = \frac{x_2 + 1}{x_1}, \quad x_4 = \frac{x_1 + x_2 + 1}{x_1 x_2} \quad \text{and} \quad x_5 = \frac{x_1 + 1}{x_2}.$$

These are well-known as the five cluster variables appearing in the simplest non-trivial cluster algebra: the cluster algebra of type A_2 . As we recall in Sect. 3, the associated *cluster variety* is an affine surface $U \subset \mathbb{A}^5$ whose coordinate ring is generated by x_1, \dots, x_5 and can be realised as the interior of the log Calabi–Yau pair (X, D) , where $X \subset \mathbb{P}^5$ is a del Pezzo surface of degree 5 and $D = \sum_{i=1}^5 D_i$ is an anticanonical pentagon of (-1) -curves. The variety U is known to be self-mirror [17, Example 5.9], i.e. the mirror U^* is isomorphic to U . In terms of the conjecture mentioned above, this mirror correspondence places the five boundary components D_i in a natural one-to-one correspondence with the five cluster variables x_i .

¹ Recall that a Fano 3-fold of type V_{12} is obtained by taking the intersection of the orthogonal Grassmannian $OGr(5, 10) \subset \mathbb{P}^{15}$ in its spinor embedding with a linear subspace of codimension 7.

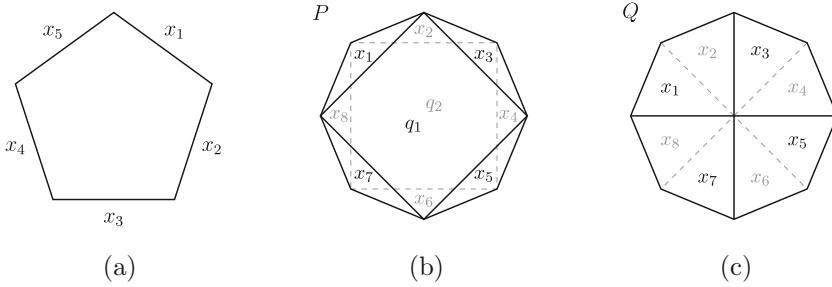


Fig. 1. The correspondence between boundary divisors and theta functions on the mirror for **a** del Pezzo surface X of degree 5, **b** the Fano 3-fold X_P of type V_{12} and **c** the Fano 3-fold X_Q of type V_{16}

The mirror of a complex projective Fano variety is expected to be a *Landau–Ginzburg model* (V, w) , i.e. a quasiprojective algebraic variety V over \mathbb{C} equipped with a holomorphic surjective function $w : V \rightarrow \mathbb{C}$, called a *Landau–Ginzburg potential*. Therefore, for our log Calabi–Yau variety U , adding the boundary divisor D to obtain the del Pezzo surface X corresponds to decorating the mirror $U^* \cong U$ with a holomorphic function. In this case, summing the five cluster variables that correspond to the components of D defines a potential $w = x_1 + \dots + x_5$ for a Landau–Ginzburg model $w : U \rightarrow \mathbb{C}$ which is mirror to X .

1.2.2. Dimension 3 and the Fano 3-fold V_{12} In dimension 3 the recurrence relation (LR_3) generates an 8-periodic sequence $(x_i : i \in \mathbb{Z}/8\mathbb{Z})$. Expanding in terms of x_1, x_2, x_3 we have

$$\begin{aligned}
 x_4 &= \frac{x_2 + x_3 + 1}{x_1} & x_5 &= \frac{(x_1 + 1)(x_3 + 1) + x_2}{x_1 x_2} \\
 x_6 &= \frac{(x_1 + x_2 + 1)(x_2 + x_3 + 1)}{x_1 x_2 x_3} \\
 x_7 &= \frac{(x_1 + 1)(x_3 + 1) + x_2}{x_2 x_3} & \text{and } x_8 &= \frac{x_1 + x_2 + 1}{x_3}.
 \end{aligned}$$

These rational functions satisfy eight relations of the form $x_{i-1}x_{i+2} = 1 + x_i + x_{i+1}$ and we observe that x_1, \dots, x_8 satisfy two further relations: $x_1x_5 = x_3x_7$ and $x_2x_6 = x_4x_8$. In analogy to the dimension 2 case, we will see in Sect. 4 that the ring generated by the eight variables x_1, \dots, x_8 defines an algebraic variety $U \subset \mathbb{A}^8$ which is also a kind of cluster variety (in the sense of Definition 2.6(3)). This variety U is the interior of a log Calabi–Yau pair (X_P, D_P) , where X_P is a special (non- \mathbb{Q} -factorial) Fano 3-fold of type V_{12} and $D_P \in |-K_X|$ is a boundary divisor with ten components. Eight components are isomorphic to \mathbb{P}^2 , two components are isomorphic to $\mathbb{P}^1 \times \mathbb{P}^1$ and they meet along their toric boundary strata according to the polytope P shown in Fig. 1b.

Like the affine del Pezzo surface before it, we will see that this 3-fold U is also self-mirror. However, in contrast to the two dimensional case, there is now a problem: we have ten boundary divisors but only eight cluster variables. Moreover

the Landau–Ginzburg model $w_P : U \rightarrow \mathbb{C}$ defined by the potential $w_P := x_1 + \dots + x_8$ does not have the right period sequence to be a mirror for a Fano 3-fold of type V_{12} . Instead the period sequence of w_P suggests that it is a mirror to a Fano 3-fold of type V_{16} (cf. Sect. 4.4.1).

The explanation for this difference is that the eight \mathbb{P}^2 components of D_P correspond to the eight cluster variables x_i , but the two $\mathbb{P}^1 \times \mathbb{P}^1$ components correspond to two ‘missing’ cluster variables

$$q_1 = x_1 x_5 - 1 = \frac{(x_1 + 1)(x_3 + 1)}{x_2} \quad \text{and}$$

$$q_2 = x_2 x_6 - 1 = \frac{(x_1 + x_2 + x_3 + 1)(x_2 + 1)}{x_1 x_3},$$

which are invariants for the squared Lyness map σ_3^2 . The new variables q_1 and q_2 appear in the derivation of a cluster algebra-like exchange graph for U (cf. Sect. 4.2.2). Adjoining q_1 and q_2 to the ring $\mathbb{C}[X_P]$ corresponds to a birational map (an *unprojection* in the language of Miles Reid) mapping X_P onto a 3-fold X_Q

$$\psi : X_P \subset \mathbb{P}_{(x_0:x_1:\dots:x_8)}^8 \dashrightarrow X_Q \subset \mathbb{P}_{(x_0:x_1:\dots:x_8:q_1:q_2)}^{10}$$

which blows up and then contracts the two (non-Cartier) Weil divisors in the boundary of X_P corresponding to q_1 and q_2 . This extends to a birational map of pairs $\psi : (X_P, D_P) \dashrightarrow (X_Q, D_Q)$, where X_Q is a degenerate Fano 3-fold of type V_{16} and D_Q is an anticanonical boundary divisor with eight $\mathbb{P}^1 \times \mathbb{P}^1$ components meeting according to the polytope Q displayed in Fig. 1c.

Finally, summing the ten cluster variables that generate the coordinate ring of X_Q gives a potential $w_Q := x_1 + \dots + x_8 + q_1 + q_2$ for a Landau–Ginzburg model $w_Q : U \rightarrow \mathbb{C}$ with the correct period sequence to be mirror to a Fano 3-fold of type V_{12} . Thus in this example the Landau–Ginzburg model (U, w_P) is mirror to the Fano variety X_Q and the Landau–Ginzburg model (U, w_Q) is mirror to the Fano variety X_P .

1.2.3. Generalising Borisov–Batyrev duality We note that the two polytopes P and Q appearing in Fig. 1 are combinatorially dual to one another. We will go one step further and interpret them as dual reflexive polytopes in the *tropicalisation* of U , a self-dual integral affine manifold with singularities, which we denote by N_U . This duality can then be generalised for any pair of dual reflexive polytopes in N_U and is the analogue of Borisov–Batyrev duality in the ordinary toric setting.

1.3. Summary

1.3.1. Contents In Sect. 2 we give a brief overview of mirror symmetry for log Calabi–Yau varieties, which is intended as motivational context for the rest of the paper. In particular we explain how to construct the *tropicalisation* N_U of a log Calabi–Yau variety U which is an integral affine manifold with singularities. We explain how to construct polytopes inside this space N_U and how they can be

dualised to give polytopes in N_V , a dual integral affine manifold with singularities corresponding to the mirror log Calabi–Yau variety $V = U^*$.

In Sect. 3 we discuss the well-known affine del Pezzo surface U of degree 5 related to the 2-dimensional Lyness recurrence (LR₂). In particular we describe the cluster structure on U , the tropicalisation N_U and we show that N_U is self-dual as an integral affine manifold with singularities. We then give some examples of mirror symmetry for pairs of reflexive polygons in N_U . In Sect. 4 we repeat all of this to do a similar analysis for the affine 3-fold of type V_{12} related to the 3-dimensional Lyness recurrence (LR₃).

1.3.2. The significance of being self-mirror Assuming the Strominger–Yau–Zaslow conjecture, a log Calabi–Yau variety U and its mirror U^* are fibred by dual Lagrangian tori. Since real 2-tori are self-dual, every log Calabi–Yau surface is diffeomorphic to its mirror, and thus the fact that the affine del Pezzo surface $U = X \setminus D$ of Sect. 1.2.1 is self-mirror is not that surprising. In fact, all maximal positive log Calabi–Yau surfaces are deformation equivalent to their mirror [22]. However, for a higher dimensional log Calabi–Yau variety to be self-mirror is unusual, and even in dimension 3 not many examples are known. Thus, from the point of view of mirror symmetry, the log Calabi–Yau 3-fold that we study in Sect. 4 is very special.

2. Mirror symmetry and log Calabi–Yau varieties

This section is intended as a motivational context for the rest of the paper and as such we refer the reader to [14, 17] for more detailed accounts.

2.1. Log Calabi–Yau varieties

Definition 2.1. A *log Calabi–Yau pair* is a pair (X, D) consisting of a smooth complex projective variety X and a reduced effective integral anticanonical divisor $D \in |-K_X|$ with simple normal crossings.² We call the interior of a log Calabi–Yau pair $U = X \setminus D$ a *log Calabi–Yau variety*.

A log Calabi–Yau variety U is naturally equipped with a nonvanishing holomorphic volume form Ω_U in the following way. The boundary divisor $D = \text{div } s_X$ is cut out by a section $s_X \in H^0(X, -K_X)$ so, after restricting to U , we get the volume form $\Omega_U = (s_X|_U)^{-1} \in H^0(U, K_U)$ which has simple poles along the components of D . Since Ω_U is only determined up to rescaling by a constant, we may assume that Ω_U is normalised so that $\int_\gamma \Omega_U = 1$, where γ is the class of the

² The smoothness and simple normal crossings assumptions are made purely for simplicity. More generally one could consider (X, D) to be a pair with \mathbb{Q} -factorial divisorial log terminal singularities (although we note that the ‘natural’ compactification of the 3-fold cluster variety appearing in Sect. 4 is not \mathbb{Q} -factorial).

real n -torus which expected to be the fibre in the SYZ fibration.³ The natural framework within which we would now like to work is the category of log Calabi–Yau varieties and *volume preserving birational maps*, i.e. birational maps $\phi: U \dashrightarrow V$ such that $\phi^*\Omega_V = \Omega_U$.

Example 2.2. The prototypical example of a log Calabi–Yau variety is the algebraic torus $\mathbb{T}_N = \mathbb{C}^\times \otimes_{\mathbb{Z}} N$ associated to a lattice $N \cong \mathbb{Z}^d$. The volume form on \mathbb{T}_N is given by $\Omega_{\mathbb{T}_N} = (2\pi i)^{-d} \frac{dz_1}{z_1} \wedge \dots \wedge \frac{dz_d}{z_d}$. There are two dual lattices associated to \mathbb{T}_N : the *cocharacter lattice* N , whose points correspond to divisorial valuations along toric boundary divisors, and the *character lattice* $M = \text{Hom}(N, \mathbb{Z})$, whose points $m \in M$ correspond to monomial functions $z^m = z_1^{m_1} \dots z_d^{m_d}$ on $\mathbb{T}_N = \text{Spec } \mathbb{C}[M]$. These monomials form a natural additive basis for the coordinate ring of \mathbb{T}_N .

Note that the roles of the two lattices N and M are interchanged when we replace the torus \mathbb{T}_N by its dual (or ‘mirror’) torus \mathbb{T}_M . A key idea of Gross, Hacking & Keel is that one can introduce an object that serves as a generalisation of the cocharacter lattice for an arbitrary log Calabi–Yau variety.

Definition 2.3. Given a log Calabi–Yau variety U with volume form Ω_U , the set of *integral tropical points* of U is given by

$$N_U(\mathbb{Z}) = \{\text{divisorial valuations } \nu: \mathbb{C}(U) \setminus \{0\} \rightarrow \mathbb{Z} \text{ such that } \nu(\Omega_U) < 0\} \cup \{0\}.$$

The set $N_U(\mathbb{Z})$ is more commonly referred to as $U^{\text{trop}}(\mathbb{Z})$ in the literature, but our notation is chosen to emphasise the fact that $N_U(\mathbb{Z})$ is supposed to be a generalisation of the cocharacter lattice N when $U = \mathbb{T}_N$. Indeed, as a set we have that $N_{\mathbb{T}_N}(\mathbb{Z}) = N$.

2.1.1. The conjecture of Gross, Hacking & Keel Gross, Hacking & Keel have conjectured that an analogue for the character lattice also exists for U , which generalises the duality enjoyed by tori to pairs of mirror log Calabi–Yau varieties. Before stating their conjecture we need to introduce two technical hypotheses.

Definition 2.4. Let (X, D) be a d -dimensional log Calabi–Yau pair with interior $U = X \setminus D$. We call U *positive* if D supports an ample divisor and we say that U has *maximal boundary* if D contains a 0-stratum (i.e. a point at which d components of D meet transversely).

From now on we will assume that all log Calabi–Yau varieties are positive and have maximal boundary. The assumption that U is positive is useful because it implies that U is affine. The maximal boundary condition is introduced to ensure that the set of integral tropical points $N_U(\mathbb{Z})$ is as big as possible. In Sect. 2.3.1 we will realise $N_U(\mathbb{Z})$ as the set of integral points in a real affine manifold with singularities N_U . In general, the dimension of N_U will be equal to the codimension of the smallest stratum of D .

³ Explicitly, fixing local coordinates z_1, \dots, z_n in the neighbourhood of a 0-stratum $p \in D \subset X$ so that $D = \mathbb{V}(z_1 \dots z_n)$, then $\gamma = \{(z_1, \dots, z_n) : |z_1| = \dots = |z_n| = \varepsilon\}$ for $0 < \varepsilon \ll 1$. This gives a well-defined class $[\gamma] \in H_n(X, \mathbb{C})$, and the fact that it is independent of the choice of p follows from [21, Theorem 10].

Conjecture 2.5. ([12, Conjecture 0.6], cf. [14, 17]) Given a positive log Calabi–Yau variety U with maximal boundary, then there exists a mirror positive log Calabi–Yau variety V with maximal boundary whose coordinate ring $\mathbb{C}[V]$ has an additive basis

$$\mathcal{B}_V = \{\vartheta_n \in \mathbb{C}[V] : n \in N_U(\mathbb{Z})\}$$

parameterised by the integral tropical points of U . The elements of this basis are called the *theta functions* of V and are canonically determined up to multiplication by scalars. The multiplication rule for theta functions $\vartheta_a \vartheta_b = \sum_{c \in N_U} \alpha_{abc} \vartheta_c$ has structure constants α_{abc} which can be obtained as certain counts of rational curves in U .

Without fixing a complexified Kähler form on U , the mirror variety V is not expected to be unique. Indeed, since changing the choice of complexified Kähler form on U corresponds to changing the complex structure on V , the variety V should appear as a fibre in a deformation family of mirrors to U . On this level, mirror symmetry is then an involution in the sense that the mirror of V is a family of log Calabi–Yau varieties deformation equivalent to U . If U and V are a pair of mirror log Calabi–Yau varieties as in the statement of the conjecture then let us write $M_U(\mathbb{Z}) := N_V(\mathbb{Z})$ and $M_V(\mathbb{Z}) := N_U(\mathbb{Z})$ (indicating that $N_V(\mathbb{Z})$ is supposed to be a generalisation of the character lattice for U , and vice-versa).

2.2. Cluster varieties

2.2.1. Toric models We can create new examples of log Calabi–Yau varieties from a given log Calabi–Yau pair (X, D) by considering volume preserving blowups of X .

Definition 2.6. Consider a log Calabi–Yau pair (X, D) with boundary divisor $D = \sum_{i=1}^k D_i$ and interior $U = X \setminus D$.

1. A *toric blowup* of (X, D) is a blowup of X along a stratum of D . A *nontoric blowup* of (X, D) is a blowup of X along a smooth subvariety $Z \subset X$ of codimension 2, where Z is contained in one of the boundary components $Z \subset D_i$ and meets the other components of D transversely.
2. We call a log Calabi–Yau pair (X, D) a *toric model* for U if there exists a map $\pi : (X, D) \rightarrow (T, B)$ to a toric pair (T, B) where π is a composition of nontoric blowups.
3. We call U a (*generalised*) *cluster variety* if it has a toric model.

We use the terminology ‘*generalised cluster variety*’ since the more commonly accepted definition of a cluster variety (cf. [17, Definition 3.1]) imposes a second condition: in addition to the toric model $\pi : (X, D) \rightarrow (T, B)$, the variety U is required to have a nondegenerate holomorphic 2-form $\sigma \in H^0(X, \Omega_X^2(\log D))$. The existence of this 2-form σ imposes a very strong condition on types of centre $Z \subset T$ that can be blown up by π . In particular it forces $Z = \bigcup_{i=1}^k Z_i$ to be a union of *hypertori*. If we let N and M be the (co)character lattices of the torus $\mathbb{T} = T \setminus B$,

then a hypertorus is a subvariety of T of the form $Z_i = \mathbb{V}(z^{m_i} + \lambda_i) \subset B_{n_i}$, where $\lambda_i \in \mathbb{C}^\times$ is some coefficient (usually assumed to be chosen generically), $n_i \in N$ determines the boundary divisor $B_{n_i} \subset T$ containing Z_i and $m_i \in n_i^\perp \subset M$. Thus the centres Z_i are determined by pairs $(n_i, m_i) \in N \times M$. The advantage of this more restrictive situation is that there is a very simple candidate for the mirror to U , called the *Fock–Goncharov dual* of U : for each $i = 1, \dots, k$ we simply swap the roles of $n_i \in N$ and $m_i \in M$ to obtain a ‘mirror’ toric model.

Nevertheless, as we will soon see, the cluster algebra-like combinatorics of seeds and mutation can be used to describe any log Calabi–Yau variety with a toric model, and do not rely on the 2-form σ . This fact has led Corti to suggest that this should be the ‘true’ definition of a cluster variety.

Remark 2.7. The name ‘generalised cluster variety’ is not ideal, since there are many other proposals for a ‘generalised cluster variety’ appearing in the literature. Of these, it is perhaps closest in spirit to the definition of a *Laurent phenomenon algebra* given by Lam and Pylyavskyy [23]. Translated into our language, a Laurent phenomenon algebra is essentially the coordinate ring of a d -dimensional log Calabi–Yau variety with a toric model given by blowing up d centres $Z_i \subset H_i \subset \mathbb{A}^d$, one in each of the coordinate hyperplanes H_i of \mathbb{A}^d .

2.2.2. Mutations A toric model $\pi : (X, D) \rightarrow (T, B)$ for U is determined by a set of centres

$$S = \{Z_i \subset T : i = 1, \dots, k\}$$

which comprise the locus $Z = \bigcup_{i=1}^k Z_i$ blown up by π . Note that the choice of toric model for U is not uniquely determined by the set S , since we can modify our chosen pairs (X, D) and (T, B) by compatible choices of toric blowups or blowdowns. However the set S does specify a unique torus $\mathbb{T}_S := T \setminus B$ and a volume preserving embedding $j_S := (\pi^{-1})|_{\mathbb{T}_S} : \mathbb{T}_S \hookrightarrow U$. (This inclusion of the torus \mathbb{T}_S into U is the geometric manifestation of the Laurent phenomenon for U .)

Similarly to the (strict) cluster case described above, we can represent each component of Z in the form $Z_i = Z(n_i, f_i) := \mathbb{V}(f_i) \subset B_{n_i}$, where $n_i \in N$ is a primitive vector⁴ and $f_i \in \mathbb{C}[n_i^\perp \cap M]$ is a Laurent polynomial. The difference is now that f_i is not constrained to be simply binomial.

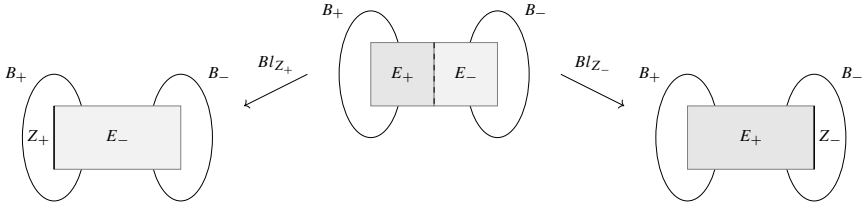
Definition 2.8. 1. We call the set S a *seed* for U and the torus embedding $j_S : \mathbb{T}_S \hookrightarrow U$ a *cluster torus chart* of U .

- Given a pair (n, f) , which represents a centre $Z = Z(n, f)$ in the boundary of a toric compactification of a torus \mathbb{T} , we define the *mutation along Z* to be the birational map $\mu_{(n,f)} : \mathbb{T} \dashrightarrow \mathbb{T}$ of the form $\mu_{(n,f)}^*(z^m) = f^{-\langle n,m \rangle} z^m$.

Example 2.9. The geometry of a mutation $\mu = \mu_{(n,f)}$ is described by Gross et al. [14, 3.1]. In particular, they show that μ can be viewed as a kind of *elementary*

⁴ If we wanted to, we could extend the definition of $Z(n_i, f_i)$ to allow arbitrary $n_i \in N$ by considering nonreduced centres $Z(n_i, f_i) = \mathbb{V}(f_i^r) \subset B_{n'_i}$, where $r \geq 1$ and $n_i = rn'_i$ for a primitive vector $n'_i \in N$.

transformation of \mathbb{P}^1 -bundles. Indeed, by blowing up if necessary, we can arrange for T to contain the two boundary divisors $B_+ := B_n$ and $B_- := B_{-n}$ and then consider the toric subvariety $T_0 \cong (\mathbb{P}^1 \times (\mathbb{C}^\times)^{d-1}) \subset T$ consisting of the big open torus \mathbb{T} and the relative interior of B_+ and B_- . Let $Z_+ = Z(n, f)$ and let $E_- := \mathbb{V}(f) \subset T_0$. Then they show that the extension of μ to a birational map $\mu: T_0 \dashrightarrow T_0$ is resolved by blowing up the locus $Z_+ \subset B_+$ and contracting the strict transform of the divisor E_- to the locus $Z_- = Z(-n, f) \subset B_-$.



Changing coordinates so that $n = (1, 0, \dots, 0)$, then μ can be assumed to be of the form

$$\mu^*(z_1, z_2, \dots, z_d) = \left(f(z_2, \dots, z_d)^{-1} z_1, z_2, \dots, z_d \right).$$

It is convenient to introduce $z'_1 = z_1^{-1} f(z_2, \dots, z_d)$ and to distinguish the domain and codomain of $\mu: \mathbb{T} \dashrightarrow \mathbb{T}'$ so that $\mathbb{T} = (\mathbb{C}^\times)_{z_1, z_2, \dots, z_d}^d$, $\mathbb{T}' = (\mathbb{C}^\times)_{z'_1, z_2, \dots, z_d}^d$ and $\mu^*(z'_1, z_2, \dots, z_d) = (z_1^{-1}, z_2, \dots, z_d)$. However note that this map is *volume negating*, in the sense that $\mu^* \Omega_{\mathbb{T}'} = -\Omega_{\mathbb{T}}$, so the torus \mathbb{T}' should be considered to come equipped with the negative of its standard volume form. Now $U = Bl_{Z_+} T_0 \setminus (B_+ \cup B_-)$ is the affine variety

$$U = \mathbb{V}(z_1 z'_1 - f(z_2, \dots, z_d)) \subset \mathbb{A}_{z_1, z'_1}^2 \times (\mathbb{C}^\times)_{z_2, \dots, z_d}^{d-1}$$

and this is covered, up to the complement of a subset $\Sigma = \mathbb{V}(z_1, z_2, f) \subset U$ of codimension two in U , by the two torus charts $\mathbb{T}, \mathbb{T}' \hookrightarrow U$ which are glued together by μ . The locus $\Sigma \subset U$ not covered by the two torus charts is the intersection of the two divisors $\Sigma = E_+ \cap E_-$, although since U is normal and affine we have that $U = \text{Spec } H^0(U \setminus \Sigma, \mathcal{O}_{U \setminus \Sigma})$, so these two charts provide enough information to recover U .

Mutating a seed Example 2.9 gives a complete description of the cluster structure for a log Calabi–Yau variety U which is determined by a seed $S = \{Z(n, f)\}$ with only one centre. In particular there are two cluster torus charts $\mathbb{T}_S = \mathbb{T}$ and $\mathbb{T}_{S'} = \mathbb{T}'$ where S' is the seed $S = \{Z(-n, f)\}$, and the mutation $\mu: \mathbb{T}_S \dashrightarrow \mathbb{T}_{S'}$ provides the transition map between them.

In general, for a seed with several centres $S = \{Z_i = Z(n_i, f_i) : i \in \{1, \dots, k\}\}$ we can consider applying a mutation $\mu_i = \mu_{(n_i, f_i)}$ for each $i \in \{1, \dots, k\}$. For a given i , we can define a new seed $\mu_i S$, such that the mutation becomes a map of cluster torus charts $\mu_i: \mathbb{T}_S \dashrightarrow \mathbb{T}_{\mu_i S}$. To do this, extend μ to a birational map of

projective toric varieties $\mu: (T, B) \dashrightarrow (T', B')$. The *mutated seed* is the set of centres $\mu_i S = \{\mu_i Z_j : j \in 1, \dots, k\}$, such that

$$\mu_i Z_j = \begin{cases} Z(-n_i, f_i) & j = i \\ C_{Z_j T'} & j \neq i \end{cases}$$

where $C_{Z_j T'} = \overline{\mu_i(\eta_{Z_j})}$ denotes the centre of Z_j on T' (the closure of the image of the generic point η_{Z_j} under μ_i). As μ_i is volume preserving, it follows that $C_{Z_j T'}$ is contained in the boundary of T' and is guaranteed to have the form $\mu_i Z_j = Z(n'_j, f'_j)$ for some $n'_j \in N$ and $f'_j \in \mathbb{C}[n'_j \cap M]$.

The exchange graph of U The *exchange graph* for U is the k -regular graph whose set of vertices is the set of seeds for U and whose set of edges is given by mutations.

An atlas of torus charts for U We can think of the set of seeds for U as giving an atlas of cluster torus charts $j_S: \mathbb{T}_S \hookrightarrow U$ which can be glued together by transition maps which are the mutations. By [14, Proposition 2.4], from any initial seed S we can consider the scheme

$$U^0 = \mathbb{T}_S \cup \bigcup_{i=1}^k \mathbb{T}_{\mu_i S}$$

obtained by gluing all the cluster tori which are one mutation away from S . In general there are some issues with this construction. In particular, U^0 may not be separated if two centres have nonempty intersection $Z_i \cap Z_j \neq \emptyset$. However, if all of the centres Z_i are disjoint then the maps $j_{\mu_i S}: \mathbb{T}_{\mu_i S} \hookrightarrow U$ glue to give an embedding $j: U^0 \hookrightarrow U$, which covers U up to a set $\Sigma = U \setminus U^0$ of codimension at least 2 [14, Lemma 3.5]. If U is positive (and hence affine) then we have $U = \text{Spec } H^0(U^0, \mathcal{O}_{U^0})$ as in Example 2.9.

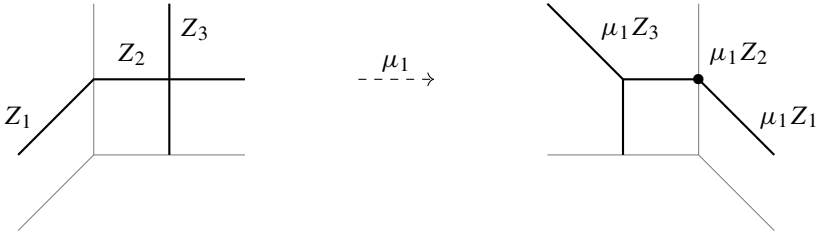
2.2.3. Examples It is natural to wonder whether there is a more explicit combinatorial formula describing the effect of a mutation μ_i on the set of pairs (n_j, f_j) that define the other centres $Z_j = Z(n_j, f_j)$ in the seed, as there is in the ordinary cluster case [14, Equation 2.3]. Unfortunately, at this level of generality the mutations are somewhat more complicated to keep track of, and the location of the centre $\mu_i Z_j$ depends crucially on the exact form of f_i and f_j . It is natural to hope that if $Z_j \subset B_{n_j}$, then $\mu_i Z_j \subset \mu_i B_{n_j}$, i.e. that Z_j remains in the same boundary component after the mutation. However this is not necessarily the case. We give a couple of examples to see the kind of difficulties that can occur.

Definition 2.10. Consider a seed $S = \{Z_1, \dots, Z_k\}$, a choice of mutation μ_i and a centre Z_j with $j \neq i$. We say that Z_j makes an *unexpected jump* if $\mu_i Z_j \not\subset \mu_i B_{n_j}$.

Example 2.11. We consider a toric model $\pi: (X, D) \rightarrow (\mathbb{A}^3, B)$ obtained by blowing up three centres which are contained in the coordinate hyperplanes of \mathbb{A}^3 :

$$\begin{aligned} Z_1 &= Z((1, 0, 0), 1 + z_2), & Z_2 &= Z((0, 0, 1), 1 + z_2), \\ Z_3 &= Z((0, 0, 1), 1 + z_1). \end{aligned}$$

Consider the mutation along Z_1 . From the geometric description given above, μ_1 blows up Z_1 and contracts the strict transform of the divisor $E_1 = \mathbb{V}(1 + z_2) \subset \mathbb{A}^3$ to the centre $\mu_1 Z_1 = Z((-1, 0, 0), 1 + z_2)$ at infinity. Since $\mu_1^*(1 + z_1^{-1} + z_2) = (1 + z_1^{-1})(1 + z_2)$, it is also straightforward to see that the mutation sends Z_3 to $\mu_1 Z_3 = Z((0, 0, 1), 1 + z_1^{-1} + z_2)$. However, since $Z_2 \subset E_1$, the contraction of the strict transform of E_1 moves the centre of Z_2 out of the divisor $B_{(0,0,1)}$. We get $\mu_1 Z_2 = Z((-1, 0, 1), 1 + z_2)$ and thus Z_2 makes an unexpected jump. We illustrate the effect of the mutation on the centres in the following diagram, where the centres Z_i have been drawn ‘tropically’.



The bad behaviour demonstrated in Example 2.11 looks like it can be fixed by introducing a generic coefficient $\lambda \in \mathbb{C}^\times$ and deforming the centre Z_2 to $Z((0, 0, 1), \lambda + z_2)$. Then we will no longer have the inclusion $Z_2 \subset E_1$ and the mutation μ_1 will keep Z_2 and Z_3 inside the same boundary component. Unfortunately, as we show in the next example, it is not always possible to avoid unexpected jumps, even if we start from a seed where all of the centres have generic coefficients.

Example 2.12. Consider the toric model $\pi : (X, D) \rightarrow (\mathbb{A}^3, B)$ obtained by blowing up three centres

$$\begin{aligned} Z_1 &= Z((1, 0, 0), a_1 + a_2 z_2 + a_3 z_3), \\ Z_2 &= Z((0, 1, 0), b_1 z_1 + b_2 + b_3 z_3), \\ Z_3 &= Z((0, 0, 1), c_1 z_1 + c_2 z_2 + c_3) \end{aligned}$$

where $a_i, b_i, c_i \in \mathbb{C}^\times$ are generic coefficients. This seed consists of three general lines, one in each of the three coordinate hyperplanes of \mathbb{A}^3 . We can apply the mutation μ_1 along Z_1 to obtain a new seed:

$$\begin{aligned} Z'_1 &:= \mu_1 Z_1 = Z((-1, 0, 0), a_1 + a_2 z_2 + a_3 z_3), \\ Z'_2 &:= \mu_1 Z_2 = Z((0, 1, 0), b_1(a_1 + a_3 z_3) + z_1^{-1}(b_2 + b_3 z_3)), \\ Z'_3 &:= \mu_1 Z_3 = Z((0, 0, 1), c_1(a_1 + a_2 z_2) + z_1^{-1}(c_2 z_2 + c_3)). \end{aligned}$$

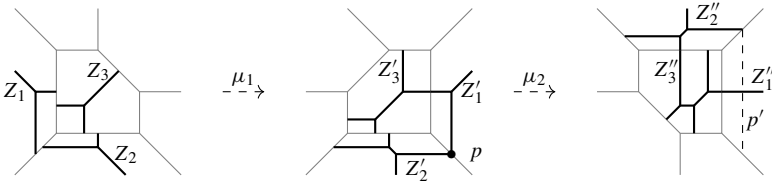
We note that Z'_1 and Z'_2 intersect in a point $p = \mathbb{V}(z_1^{-1}, z_2, a_1 + a_3 z_3)$ belonging to the intersection of their boundary components. If we now apply the mutation μ_2 along Z'_2 then we compute that the total transform of the centre Z'_1 is reducible and given by

$$Z((-1, 0, 0), z_2^{-1} + a_2 b_1) \cup Z((-1, 0, 0), a_1 + a_3 z_3)$$

where the first component is the centre $\mu_2 Z'_1$ and the second component is the exceptional line p' over the point p (represented by the dashed vertical line in the third diagram below). Therefore mutating the seed at Z'_2 gives

$$\begin{aligned} Z''_1 &:= \mu_2 Z'_1 = Z((-1, 0, 0), z_2^{-1} + a_2 b_1), \\ Z''_2 &:= \mu_2 Z'_2 = Z((0, -1, 0), b_1(a_1 + a_3 z_3) + z_1^{-1}(b_2 + b_3 z_3)), \\ Z''_3 &:= \mu_2 Z'_3 = Z((0, 0, 1), (a_2 c_1 + c_2 z_1^{-1})(a_1 b_1 + b_2 z_1^{-1}) + z_2^{-1}(a_1 c_1 + c_3 z_1^{-1})). \end{aligned}$$

We draw the sequence of mutations with the centres represented tropically, as before.



We now see that Z''_1 is contained in the hypersurface determined by the equation of Z''_3 and so, in exactly the same style as Example 2.11, if we mutate this last seed at Z''_3 then Z''_1 will make an unexpected jump.

2.3. The tropicalisation of a log Calabi–Yau variety

2.3.1. The tropicalisation of U The cocharacter lattice of a torus comes with some extra structure that we would like to generalise to $N_U(\mathbb{Z})$. There is no group structure on $N_U(\mathbb{Z})$ in general. Instead (as hinted above) the right way to proceed is to try and realise $N_U(\mathbb{Z})$ as the integral points of a real affine manifold N_U , in the same way that the lattice N can be realised as the set of integral points of the real vector space $N_{\mathbb{R}} := N \otimes_{\mathbb{Z}} \mathbb{R}$. This can be done, but only by introducing singularities into the affine structure on N_U . The space N_U thus obtained is an *integral affine manifold with singularities* and is referred to as the *tropicalisation* of U .

One can build N_U directly, by choosing a compactification⁵ (X, D) of U and defining N_U to be the cone over the dual intersection complex of the boundary divisor D [17]. However, for log Calabi–Yau varieties with a toric model $\pi : (X, D) \rightarrow (T, B)$ then, by generalising the 2-dimensional case covered in [12, 1.2], there is a natural way to build the space N_U by altering the affine structure on the cocharacter space $N_{\mathbb{R}}$ of the torus $\mathbb{T}_S = T \setminus B$. In particular, if U has a toric model then, as a real manifold, N_U is homeomorphic to $N_{\mathbb{R}} \cong \mathbb{R}^d$.

For simplicity (and because it applies in the case we study later on) we assume that (X, D) and (T, B) are smooth, and the centres $Z_i \subset T$ blown up by π are

⁵ Despite the potentially misleading notation, in dimension $d \geq 3$ the construction of N_U is actually dependent on the choice of a compactification (X, D) of U . Different choices of compactification lead to affine structures on N_U which differ up to integral piecewise-linear homeomorphism, cf. [17, Definition 3.8].

smooth and disjoint. Let \mathcal{F} be the fan in $N_{\mathbb{R}}$ that defines (T, B) and consider a pair of maximal smooth cones σ_1, σ_2 of \mathcal{F} that meet along a codimension 2 face $\tau = \sigma_1 \cap \sigma_2$. We can write $\sigma_1 = \langle v_1, \dots, v_d \rangle$, $\sigma_2 = \langle v_2, \dots, v_{d+1} \rangle$ and $\tau = \langle v_2, \dots, v_d \rangle$ for some choice of primitive vectors $v_1, \dots, v_{d+1} \in N$. Now the cone τ corresponds to a torus invariant curve $\overline{C}_\tau \cong \mathbb{P}^1 \subset T$ and therefore also a curve $C_\tau = \pi^{-1}(\overline{C}_\tau)$ in the boundary of (X, D) . Similarly the vectors v_i correspond to the set of boundary divisors $D_i = D_{v_i} \subset D$ meeting C_τ . Consider the linear map $\psi: \sigma_1 \cup \sigma_2 \rightarrow \mathbb{R}^d$ defined by

$$\psi(v_i) = e_i \text{ for } i = 1, \dots, d, \quad \text{and} \quad \psi(v_{d+1}) = -e_1 - \sum_{i=2}^d (D_i \cdot C_\tau) e_i,$$

where e_1, \dots, e_d are the standard basis vectors of \mathbb{R}^d . This sends σ_1 onto the positive orthant $\sigma'_1 \subset \mathbb{R}^d$ and σ_2 onto an appropriately chosen cone $\sigma'_2 \subset \mathbb{R}^d$, which has been cooked up so that the toric variety defined by the fan with the two maximal cones σ'_1, σ'_2 contains a projective curve, $C_{\tau'}$ for $\tau' = \sigma'_1 \cap \sigma'_2$, which has identical intersection numbers with boundary divisors as the curve $C_\tau \subset X$.

To define the tropicalisation N_U we let N_U^{sing} be the union of cones of \mathcal{F} of codimension ≥ 2 and $N_U^0 = N_U \setminus N_U^{\text{sing}}$. To define the affine structure on N_U^0 , for any pair of maximal cones σ_1, σ_2 in \mathcal{F} as above we consider the integral affine structure on $\text{int}(\sigma_1 \cup \sigma_2)$ given by pulling back the integral affine structure on \mathbb{R}^d by the map $\psi|_{\text{int}(\sigma_1 \cup \sigma_2)}$. In particular, we have the following condition, in terms of the intersection theory on X , to tell when a piecewise linear function is actually linear along some codimension 2 cone of \mathcal{F} [24, 1.3]. Suppose that $\phi: \text{int}(\sigma_1 \cup \sigma_2) \rightarrow \mathbb{R}$ is a piecewise-linear function which is linear on each of the cones σ_1, σ_2 . This determines a Weil divisor $\Xi_\phi = \sum_{i=1}^{d+1} \phi(v_i) D_{v_i}$ on X . Then ϕ is linear along the interior of $\tau = \sigma_1 \cap \sigma_2$ if $\Xi_\phi \cdot C_\tau = 0$.

The sets of the form $\text{int}(\sigma_1 \cup \sigma_2)$ cover N_U^0 , and these glue together to give an affine structure on N_U^0 . It may or may not be possible to extend this over some, or all, of the cones of N_U^{sing} , so at this point it is customary to redefine N_U^0 to be the maximal subset of N_U on which this affine structure extends and then set $N_U^{\text{sing}} = N_U \setminus N_U^0$. We call N_U^{sing} the *singular locus* of N_U . We note that the subset of integral tropical points $N_U(\mathbb{Z}) \subset N_U$ is identified with the cocharacter lattice $N \cong \mathbb{Z}^d$ of $N_{\mathbb{R}}$ by this construction.

2.3.2. Scattering diagrams Given a log Calabi–Yau variety U , the approach pioneered in [12] to proving Conjecture 2.5 in the 2-dimensional setting is to construct the ring $\mathbb{C}[V]$ directly from the tropicalisation N_U , by equipping N_U with the structure of a *consistent scattering diagram*.

We begin by working in $N_{\mathbb{R}}$, where $N = \mathbb{Z}^d$ is a lattice with dual lattice $M = \text{Hom}(N, \mathbb{Z})$. In general, one has to be able to work with formal power series that have exponents in N , for example by choosing a strictly convex cone $\sigma \subset N$ and working with the ring $\mathbb{C}[[\sigma \cap N]]$ (or else by introducing some formal parameters to control the convergence). Let $\mathfrak{m} \subset \mathbb{C}[[\sigma \cap N]]$ denote the maximal ideal. A *wall* in $N_{\mathbb{R}}$ is a rational polyhedral cone $\mathfrak{d}_i \subset N_{\mathbb{R}}$ of codimension 1. Roughly speaking, a

scattering diagram is then a collection $\mathfrak{D} = \{(\partial_i, f_i) : i \in I\}$ of walls ∂_i decorated with *wall functions* f_i . If $u_i \in M$ is a primitive vector such that $\partial_i \subset u_i^\perp$, then the wall function $f_i \in \mathbb{C}[[u_i^\perp \cap \sigma \cap N]]$ is a monic power series, i.e. $f_i \equiv 1 \pmod{m}$. The collection of walls is usually not finite and may accumulate in certain regions of $N_{\mathbb{R}}$, or even all of $N_{\mathbb{R}}$. Moreover the wall functions are almost always infinite power series, rather than polynomials, in which case there is a further finiteness condition specifying that only finitely many $f_i \not\equiv 1 \pmod{m^k}$ for each $k \geq 1$. However, the scattering diagrams constructed for the examples discussed in this paper are always finite: the set of walls form a finite complete fan \mathcal{F} in $N_{\mathbb{R}}$ and the wall functions are all polynomials.

Given any $(\partial, f) \in \mathfrak{D}$, crossing the wall ∂ in the direction of the normal vector u specifies a *wall crossing automorphism*

$$\theta_{(\partial, f)} : \mathbb{C}[[\sigma \cap N]] \rightarrow \mathbb{C}[[\sigma \cap N]] \quad \theta_{(\partial, f)}(z^n) = z^n f^{-\langle n, u \rangle}.$$

The scattering diagram is then called *consistent* if, for any loop $\gamma : [0, 1] \rightarrow N_{\mathbb{R}}$ that begins and ends in a chamber of \mathfrak{D} and crosses all walls of \mathfrak{D} transversely, the composition of all the wall crossing automorphisms is the identity.⁶

Log Calabi–Yau varieties with a toric model Suppose that U is log Calabi–Yau variety with a toric model $\pi : (X, D) \rightarrow (T, B)$ determined by a seed $S = \{Z_i : i = 1, \dots, k\}$, where each Z_i is a general smooth hypersurface in a component of B . Let N be the cocharacter lattice of the torus $T \setminus B$. Under these assumptions Argüz and Gross [2] give a general inductive method to construct a consistent scattering diagram \mathfrak{D}_S in $N_{\mathbb{R}}$. They define an initial scattering diagram $\mathfrak{D}_{S, \text{in}}$ which is supported on the walls of the fan of T which are affected by the nontoric blowup π . Then they give an inductive procedure which can be used to compute a consistent scattering diagram \mathfrak{D}_S from $\mathfrak{D}_{S, \text{in}}$ [2, Theorem 1.1].

Broken lines In order to use $\mathfrak{D} = \mathfrak{D}_S$ to construct the coordinate ring $\mathbb{C}[V]$ of the mirror $V = U^*$, it is important to fix the integral affine structure on $N_{\mathbb{R}}$ by reconsidering \mathfrak{D} as being a scattering diagram in N_U . Now the basis of theta functions $\mathcal{B}_V = \{\vartheta_n \in \mathbb{C}[V] : n \in N_U(\mathbb{Z})\}$ of Conjecture 2.5 are computed by counting *broken lines* in N_U , which are tropicalisations of certain rational curves in U . Roughly speaking, a *broken line* for $n \in N_U(\mathbb{Z})$ which starts at $q \in N_U$ is a parameterised piecewise linear path $\ell : [0, \infty) \rightarrow N_U$ such that

1. $\ell(0) = q$,
2. ℓ is allowed to bend finitely many times as it crosses walls of \mathfrak{D} and,
3. after it makes its last bend, ℓ exits N_U with tangent vector $\ell'(t) = n$.

If we let $t_0 = 0, t_{k+1} = \infty$ and $t_1, \dots, t_k \in \mathbb{R}_{>0}$ be the times at which ℓ bends, and (∂_i, f_i) be the corresponding walls of \mathfrak{D} . Then we can associate a monomial $m_i \in \mathbb{C}[N]$ to each domain of linearity (t_i, t_{i+1}) of ℓ . This is done inductively by labelling the last domain of linearity (t_k, ∞) with $m_k := z^n$, and then labelling (t_{i-1}, t_i) with a monomial m_{i-1} appearing in the expansion of $\theta_{(\partial_i, f_i)}(m_i)$ which is dictated to us by the bend that ℓ makes along the i th wall.

⁶ This composition has to be defining inductively, working modulo successive powers of m^k , when γ crosses infinitely many walls of \mathfrak{D} .

Theta functions Fix an initial point $q \in N_U$, which is assumed to be a suitably generic (i.e. irrational) point of N_U to ensure that ℓ crosses all walls of \mathfrak{D} transversely. The theta function ϑ_n can be expanded as a Laurent power series⁷ $\vartheta_n = \sum_{\ell} m_{\ell} \in \mathbb{C}[[N]]$ obtained by taking the sum over all broken lines for n which start at q , where $m_{\ell} := m_0$ is the monomial attached to the first domain of linearity of ℓ obtained by the process described above. These theta functions then form an additive basis for a ring which is expected to be the coordinate ring of the mirror variety $V = U^*$.

2.3.3. Generalising toric geometry Once we have constructed the mirror log Calabi–Yau variety $V = U^*$, we can treat the tropicalisations N_U and $M_U := N_V$ as an analogue of the cocharacter space and character space for U respectively. These integral affine manifolds with singularities are equipped with a dual intersection pairing and Mandel [24] has used this to generalise many of the traditional techniques of toric geometry to this setting, particularly in the 2-dimensional case.

The intersection pairing The dual intersection pairing is given by

$$\langle \cdot, \cdot \rangle : N_U(\mathbb{Z}) \times M_U(\mathbb{Z}) \rightarrow \mathbb{Z} \quad \langle n, m \rangle = \nu_{D_n}(\vartheta_m)$$

which is given by evaluating the order of vanishing of a theta function $\vartheta_m \in \mathbb{C}[U]$ along a boundary component D_n appearing in a compactification of U . This can be extended to a pairing $\langle \cdot, \cdot \rangle : N_U \times M_U \rightarrow \mathbb{R}$ by first extending to the rational points of N_U and M_U by bilinearity, and then extending to the real valued points of N_U and M_U by continuity. At least in the 2-dimensional setting, the intersection pairing obtained this way is the same the intersection pairing given by switching the roles of U and V [24, Theorem 1.5].

Convexity in N_U Given the intersection pairing, Mandel now defines the (*strong*) *convex hull* of a subset $S \subset N_U$ to be

$$\text{conv}(S) := \left\{ n \in N_U : \langle n, s \rangle \geq \inf_{s \in S} \langle s, m \rangle, \forall m \in M_U \right\}$$

and similarly for subsets of M_U . Then a (*strongly*) *convex* subset $S \subset N_U$ is a subset for which $S = \text{conv}(S)$. A *polytope* $P \subset N_U$ is the convex hull of a finite set S , and we call P *integral* if $P = \text{conv}(P \cap N_U(\mathbb{Z}))$. Moreover we can define the *Newton polytope* $\text{Newt}(\vartheta) \subset M_U$ for a function $\vartheta \in \mathbb{C}[U]$ to be

$$\text{Newt}(\vartheta) = \text{conv} \left\{ m \in M_U(\mathbb{Z}) : \vartheta = \sum_{m \in M_U} \alpha_m \vartheta_m, \alpha_m \neq 0 \right\}.$$

For any $c \in \mathbb{R}$ and any $m \in M_U$ we let $(m)^{\geq c}$ denote the ‘halfspace’ of N_U given by

$$(m)^{\geq c} := \{ n \in N_U : \langle n, m \rangle \geq c \}$$

⁷ In a general scattering diagram this expansion is only possible as a formal Laurent power series, corresponding to counts that involve infinitely many broken lines.

which, in contrast to the classical setting, may be a bounded subset of N_U , or even empty. Then the *polar polytope* of a set $S \subset M_U$ is defined to be $S^\circ := \bigcap_{s \in S} (\vartheta_s)^{\geq -1}$, and these are precisely the convex polytopes of N_U that contain the origin [24, Corollary 5.9]. Note that $(P^\circ)^\circ = P$. Finally, as in the toric setting, we can define an integral polytope $P \subset N_U$ to *reflexive* if $P^\circ \subset M_U$ is an integral polytope in M_U .

2.4. Mirror symmetry

2.4.1. Mirror symmetry for Fano varieties Let X be a smooth projective d -dimensional Fano variety over \mathbb{C} . As mentioned in the introduction Sect. 1.2.1, mirror symmetry predicts the existence of a mirror Landau–Ginzburg model (V, w) to X . Following [20, 2.1], to make the correspondence more precise we must decorate the two sides of the mirror with some extra data

$$(X, s_X, \omega_X) \xleftrightarrow{\text{mirror}} ((V, w), \Omega_V, \omega_V)$$

where ω_X and ω_V are symplectic forms, $s_X \in H^0(X, -K_X)$ is an anticanonical section and $\Omega_V \in H^0(V, K_V)$ is a volume form. In particular, the section s_X specifies a boundary divisor $D = \text{div } s_X \in |-K_X|$. In the case that (X, D) is a Fano compactification of a positive log Calabi–Yau variety $U = X \setminus D$ with maximal boundary, the mirror Landau Ginzburg model to X will be defined on the mirror to U , i.e. $V = U^*$. In terms of the mirror correspondence above, deleting the boundary divisor of X corresponds to forgetting the potential on V .

From the point of view of homological mirror symmetry, there are now various flavours of the Fukaya category and derived category that one can associate to either side of this correspondence which are conjectured to be equivalent. However we take a slightly more low-tech point of view championed by the Fanosearch program [7], as we now describe.

2.4.2. Landau–Ginzburg mirrors There is a test one can apply to check whether a given Landau–Ginzburg model (V, w) is a possible mirror to a given Fano variety X , which is to compute the (*classical*) *period* of w ,

$$\pi_w(t) = \int_V \frac{\Omega_V}{1 - tw} \in \mathbb{C}[[t]].$$

This calculation is particularly simple in the case that V has a toric model, corresponding to the inclusion of a cluster torus chart $j: \mathbb{T} \hookrightarrow V$. After restricting w to \mathbb{T} , we obtain a Laurent polynomial $w|_{\mathbb{T}} \in \mathbb{C}[x_1^{\pm 1}, \dots, x_d^{\pm 1}]$ and it follows that

$$\pi_w(t) = \pi_{w|_{\mathbb{T}}}(t) = \sum_{n=0}^{\infty} \text{const}((w|_{\mathbb{T}})^n) t^n,$$

which can be seen by expanding $(1 - tw|_{\mathbb{T}})^{-1}$ as a power series in t and repeatedly applying Cauchy’s residue theorem. Under mirror symmetry, $\pi_w(t)$ is expected to

equal the *regularised quantum period* $\widehat{G}_X(t)$ of X , which is a power series whose coefficients encode certain Gromov–Witten invariants for X (see [8, A] for details). For all of the 105 smooth 3-dimensional Fano varieties X , the regularised quantum period $\widehat{G}_X(t)$ has been computed by Coates et al. [8].

2.4.3. A generalisation of Batyrev–Borisov duality Let U and $V = U^*$ be two mirror log Calabi–Yau varieties and let $\mathcal{B}_U = \{\vartheta_m : m \in M_U\}$ and $\mathcal{B}_V = \{\varphi_m : m \in N_U\}$ be the bases of theta functions on U and V . Given a pair of dual reflexive polygons $P \subset N_U$ and $Q = P^* \subset M_U$ we can now make the following constructions, which generalise Batyrev–Borisov mirror symmetry for toric Fano varieties.⁸

1. We define a *Landau–Ginzburg model* (V, w_P) , where the potential $w_P = \sum_{p \in P} a_p \varphi_p$ is obtained by summing the theta functions on V that correspond to the integral points of P with a specific choice of coefficients $a_p \in \mathbb{Z}_{\geq 0}$ (see Remark 2.14).
2. The polytope $Q \subset M_U$ determines a grading on the ring $\mathbb{C}[U]$, where $\deg \vartheta_m$ is the least integer k such that $m \in kQ$, for each $m \in M_U(\mathbb{Z})$. We let R_Q be the homogenisation of $\mathbb{C}[U]$ with respect to this grading, with homogenising variable ϑ_0 . Let (X_Q, D_Q) be the pair $X_Q = \text{Proj } R_Q$ with boundary divisor $D_Q = \mathbb{V}(\vartheta_0)$.

Note that X_Q is an anticanonically embedded, possibly degenerate (i.e. non- \mathbb{Q} -factorial) Fano variety compactifying $U = X_Q \setminus D_Q$, where the sections of $|-K_{X_Q}|$ correspond to the integral points of Q . The expectation is that (X_Q, D_Q) and (V, w_P) are mirror in the following sense.

Conjecture 2.13. If (X_Q, D_Q) admits a \mathbb{Q} -Gorenstein deformation to a pair (X, D) , where X is a \mathbb{Q} -factorial Fano variety, then there exists a choice of positive integral coefficients on the lattice points of P such that the Landau–Ginzburg model (V, w_P) is mirror to (X, D) .

Note that P may admit more than one (or even no) such choice of coefficients if X_P admits more than one (or no) deformation to a Fano variety X . In general P is expected to support a Landau–Ginzburg potential corresponding to each deformation component of X_Q (cf. Example 4.17).

Remark 2.14. We should explain how to choose the coefficients a_p in the construction of the Landau–Ginzburg model (V, w_P) . In dimension $d = 2$, the *Minkowski ansatz* of the Fanosearch program [7, 6] suggests that the correct choice of coefficients on a reflexive polygon is to label the origin with coefficient $a_0 = 0$ and to label all of the other lattice points with *binomial edge coefficients*, i.e. we label the i th lattice point on each edge of lattice length k with the coefficient $\binom{k}{i}$. In higher dimensions we expect that the correct formulation will be given by a generalisation to this setting of the *0-mutable polynomials*, introduced by Corti et al. [10].

⁸ Traditionally Batyrev duality (resp. Batyrev–Borisov duality) refers to the mirror duality between the resolution of a general Calabi–Yau hypersurface (resp. complete intersection) inside two dual toric Fano varieties.

In the toric case, the 0-mutable polynomials supported on a face $F \subset P$ are special labellings of F with positive integral coefficients which are conjecturally in bijection with the smoothing components of the corresponding strata $D_F \subset X_Q$. The expectation is that the potential w_P obtained by labelling the faces of P with a compatible system of 0-mutable polynomials will then specify the deformation of X_Q described in Conjecture 2.13.

3. Dimension 2: the del Pezzo surface dP_5

As an illustration before we tackle the 3-dimensional case, we begin by briefly recalling the famous tale of the del Pezzo surface dP_5 .

3.1. The affine del Pezzo surface U

Let x_1, \dots, x_5 be the five terms of the 2-dimensional Lyness recurrence (LR₂) given in Sect. 1.2.1. Geometrically, x_1, \dots, x_5 are regular functions on an affine surface

$$U = \text{Spec } \mathbb{C}[x_1, \dots, x_5] / (x_{i-1}x_{i+1} - x_i - 1 : i \in \mathbb{Z}/5\mathbb{Z}),$$

the vanishing locus of the five relations obtained from (LR₂). We can homogenise the equations with respect to a new variable x_0 to obtain the projective closure $X = \bar{U} \subset \mathbb{P}_{x_0, x_1, \dots, x_5}^5$ which is a smooth projective surface. The projection map $p_{12}: X \rightarrow \mathbb{P}_{x_0, x_1, x_2}^2$ is birational, and by resolving the base locus of p_{12}^{-1} we find that X is a blowup of \mathbb{P}^2 in four points

$$e_1 = (0 : 1 : -1), \quad e_2 = (1 : 0 : -1), \quad d_3 = (1 : 0 : 0), \quad d_5 = (0 : 1 : 0)$$

making X a del Pezzo surface of degree 5. As is classically known, there are ten (-1) -curves on X . We call them $D_1, \dots, D_5, E_1, \dots, E_5$, where E_1, E_2, D_3, D_5 are the exceptional curves over the points e_1, e_2, d_3, d_5 and the remaining six curves are the strict transform of the lines passing through any two of these four points, labelled according to Fig. 2. These ten curves have dual intersection diagram given by the Petersen graph.

A log Calabi–Yau pair (X, D) The complement to U is the divisor $D := X \setminus U$, which is an anticanonical cycle $D = \bigcup_{i=1}^5 D_i \in |-K_X|$ of five (-1) -curves, corresponding to the outside ring of the Petersen graph. In other words, U is the interior of a log Calabi–Yau pair (X, D) .

The interior (-1) -curves The other five (-1) -curves $E = \bigcup_{i=1}^5 E_i$ form a complementary anticanonical pentagram, and are called *interior* (-1) -curves. They are given by the locus in U where a cluster variable vanishes, i.e. $E_i|_U = \mathbb{V}(x_i) \subset U$ for $i = 1, \dots, 5$.

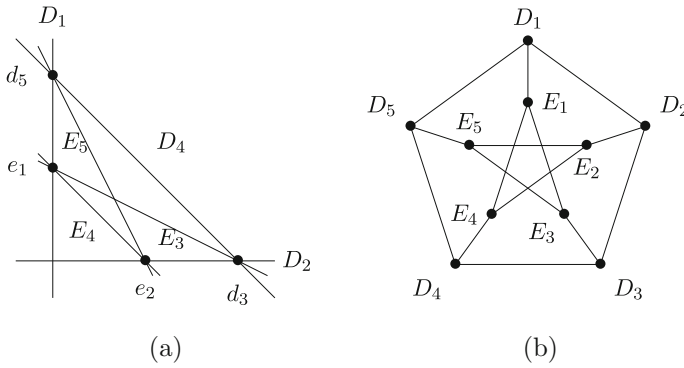


Fig. 2. a A realisation of $X \subset \mathbb{P}^5$ as a blowup of \mathbb{P}^2 . **b** The dual intersection graph of the ten (-1) -curves in X

3.2. The Grassmannian $Gr(2, 5)$

The five equations defining the affine surface U can be written as the five maximal Pfaffians of the following skewsymmetric 5×5 matrix (where, for simplicity, we have omitted the diagonal of zeroes and the antisymmetry)

$$Pf_4 \begin{pmatrix} 1 & x_1 & x_2 & 1 \\ & 1 & x_3 & x_4 \\ & & 1 & x_5 \\ & & & 1 \end{pmatrix} = 0 \implies x_{i-1}x_{i+1} = x_i + 1 \quad \forall i \in \mathbb{Z}/5\mathbb{Z}.$$

We can homogenise (LR_2) by introducing five parameters y_1, \dots, y_5 in a particularly nice and symmetric way:

$$Pf_4 \begin{pmatrix} y_5 & x_1 & x_2 & y_3 \\ & y_2 & x_3 & x_4 \\ & & y_4 & x_5 \\ & & & y_1 \end{pmatrix} = 0 \implies x_{i-1}x_{i+1} = x_i y_i + y_{i-2} y_{i+2} \quad \forall i \in \mathbb{Z}/5\mathbb{Z}. (*)$$

After setting $x_i = -1$ for all i , we see that $(y_{2i} : i \in \mathbb{Z}/5\mathbb{Z})$ is also a solution to (LR_2) .

The homogenised equations define a 7-dimensional variety $\mathcal{U} \subset \mathbb{A}^{10}$, which is the affine cone over $Gr(2, 5)$ in the Plücker embedding. The projection $p : \mathcal{U} \rightarrow \mathbb{A}_{y_1, \dots, y_5}^5$ realises \mathcal{U} as a flat family of affine del Pezzo surfaces. For any point in the big open torus $y \in (\mathbb{C}^\times)^5 \subset \mathbb{A}^5$, the fibre $U_y = p^{-1}(y)$ is isomorphic to $U = X \setminus D$ after making the change of variables $z_i = \frac{x_i y_i}{y_{i+2} y_{i-2}}$ for all $i \in \mathbb{Z}/5\mathbb{Z}$. However, above the coordinate strata of \mathbb{A}^5 the fibres begin to degenerate. The most degenerate fibre, appearing over $0 \in \mathbb{A}^5$, is the *5-vertex*

$$p^{-1}(0) = \mathbb{A}_{x_1, x_2}^2 \cup \mathbb{A}_{x_2, x_3}^2 \cup \mathbb{A}_{x_3, x_4}^2 \cup \mathbb{A}_{x_4, x_5}^2 \cup \mathbb{A}_{x_5, x_1}^2,$$

a cycle of 5 coordinate planes glued together along their toric boundary strata.

Remark 3.1. This fibration $p: \mathcal{U} \rightarrow \mathbb{A}^5$ is (very nearly) the mirror family to (X, D) constructed by Gross et al. [12], in which the variables x_1, \dots, x_5 , the compactifying parameters y_1, \dots, y_5 and the equations $(*)$ are interpreted in terms of the Gromov–Witten theory of (X, D) . Indeed, the mirror family constructed in [12] is fibred over the toric base scheme $\text{Spec } \mathbb{C}[\overline{\text{NE}}(X)]$. In terms of their construction, our parameters correspond to $y_i = z^{D_i}$, and hence our family can be viewed as a fibration over $\mathbb{A}^5 = \text{Spec } \mathbb{C}[z^{D_1}, \dots, z^{D_5}]$. In other words, their family can be pulled back from our one by the inclusion $\mathbb{C}[z^{D_1}, \dots, z^{D_5}] \hookrightarrow \mathbb{C}[\overline{\text{NE}}(X)]$.

In general, the fibres of the family \mathcal{U} are mirror to the interior of the pair (X, D) , so the fact that U appears in both roles here due to the fact that it is self-mirror.

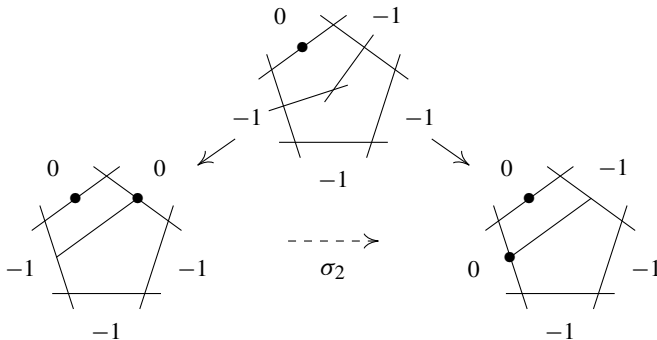
3.3. The tropicalisation of U

3.3.1. A toric model for U Consider the toric pair (T, B) obtained by blowing up the two points $d_5, d_3 \in \mathbb{P}^2$ in Fig. 2a above, so that T is a smooth projective toric surface whose boundary divisor B consists of a cycle of five rational curves, with self-intersection numbers $(0, 0, -1, -1, -1)$. This gives a toric model $\pi: (X, D) \rightarrow (T, B)$ for U which is a composition of two nontoric blowups of T (the blowup of the image of the two points $e_1, e_2 \in T$). In particular, the induced map $\pi|_D: D \rightarrow B$ on boundary divisors is an isomorphism and so we can label the components of $B = \bigcup_{i=1}^5 B_i$ by $i \in \mathbb{Z}/5\mathbb{Z}$, where $B_i = \pi(D_i)$.

The seed for this toric model is the set of points $S = \{e_1, e_2\}$, so let us denote the corresponding inclusion of a cluster torus by $j_{12}: \mathbb{T}_{12} = \text{Spec } \mathbb{C}[x_1^{\pm 1}, x_2^{\pm 1}] \hookrightarrow U$. Now the Lyness map and its inverse are given by

$$\sigma_2(x_1, x_2) = \left(x_2, \frac{1+x_2}{x_1}\right) = (x_2, x_3), \quad \sigma_2^{-1}(x_1, x_2) = \left(\frac{1+x_1}{x_2}, x_1\right) = (x_5, x_1)$$

and these are (up to a permutation of the coordinates) the mutation at $e_1 \in B_1$ and the mutation at $e_2 \in B_2$ respectively. Consider the mutation at e_1 . It is given by blowing up e_1 and contracting the strict transform of the curve E_3 to a point $e_3 \in B_3$. This gives a toric model $\pi': (X, D) \rightarrow (T', B')$ which is isomorphic to the original one, except that now all the labels have been shifted by one, $i \mapsto i + 1 \in \mathbb{Z}/5\mathbb{Z}$. In particular the dense open torus is $T' \setminus B' = \mathbb{T}_{23} = \text{Spec } \mathbb{C}[x_2^{\pm 1}, x_3^{\pm 1}]$. Thus the Lyness map can be interpreted as a mutation of toric models.



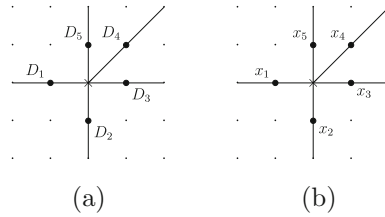


Fig. 3. **a** The fan for (X, D) in N_U . **b** The scattering diagram for U in M_U

By the five-periodicity of the Lyness map, the surface U contains five cluster torus charts $\mathbb{T}_{i,i+1} := \text{Spec } \mathbb{C}[x_i^{\pm 1}, x_{i+1}^{\pm 1}]$ for $i \in \mathbb{Z}/5\mathbb{Z}$ and U is given by the union of all five of them, identified according to the mutations.

The exchange graph of U Each toric model for U has two nontoric centres to blow up in, so the graph is 2-valent. The 5-periodicity implies that G is a pentagon.

3.3.2. The tropicalisation N_U Consider the complete fan \mathcal{F} in \mathbb{R}^2 determined by the five rays $\rho_i = \mathbb{R}_{\geq 0}v_i$ for $i \in \mathbb{Z}/5\mathbb{Z}$, where the v_i are the five points

$$v_1 = (-1, 0), \quad v_2 = (0, -1), \quad v_3 = (1, 0), \quad v_4 = (1, 1), \quad v_5 = (0, 1).$$

This is the fan of the toric pair (T, B) which appears in our toric model (Fig. 3). We can now construct N_U , the tropicalisation of U , by taking this fan \mathcal{F} and altering the integral affine structure in \mathbb{R}^2 as described in Sect. 2.3.1. This changes the affine structure along the rays ρ_1 and ρ_2 , corresponding to the two components of (T, B) along which a nontoric blowup occurs, and has the effect of bending lines that pass through ρ_1 and ρ_2 towards the origin. As a result it introduces a singularity at the origin $0 \in N_U$.

3.3.3. A scattering diagram for U The same fan \mathcal{F} in N_U also supports the structure of a scattering diagram \mathfrak{D} which can be used to construct the coordinate ring of (the mirror to) U . The construction of \mathfrak{D} and its relationship to $\mathbb{C}[U]$ is described in [12, Example 3.7]. To obtain \mathfrak{D} , we attach the following five scattering functions $f_i \in \mathbb{C}[z_1^{\pm 1}, z_2^{\pm 1}]$ to the rays ρ_i for $i \in \mathbb{Z}/5\mathbb{Z}$:

$$f_1 = 1 + z_1, \quad f_2 = 1 + z_2, \quad f_3 = 1 + z_1, \quad f_4 = 1 + z_1z_2, \quad f_5 = 1 + z_2.$$

It is now straightforward to check that the collection of walls $\mathfrak{D} = \{(\rho_i, f_i) : i \in \mathbb{Z}/5\mathbb{Z}\}$ defines a consistent scattering diagram, i.e. that starting from any point in the interior of a chamber of \mathcal{F} and composing the five wall crossing automorphisms corresponding to a loop around $0 \in N_U$ yields the identity.

To get from the scattering diagram back to $\mathbb{C}[U]$ we can consider the cluster monomials $x_i = \vartheta_{v_i}$ which are the theta functions corresponding to the points $v_i \in M_U$ for $i \in \mathbb{Z}/5\mathbb{Z}$. As described in Sect. 2.3.2 these can be expanded as Laurent polynomials $x_i = \sum_{\ell} c_{\ell} z^{\ell}$ where ℓ ranges over all of the broken lines for v_i starting at some given point $q \in N_U$. In our case the coefficients of all the scattering functions are all equal to 1 so all $c_{\ell} = 1$. Suppose that q is chosen near to

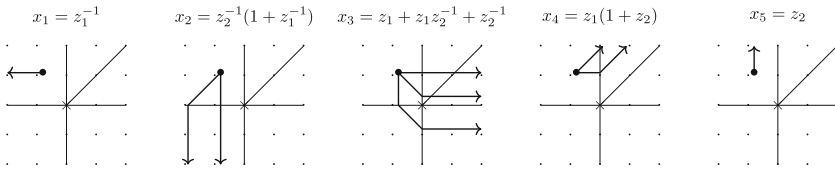


Fig. 4. The monomials x_i obtained by counting broken lines

Table 1. Table of intersection numbers $\langle D_i, x_j \rangle$ for $i, j \in \mathbb{Z}/5\mathbb{Z}$

	D_1	D_2	D_3	D_4	D_5
x_1	1	0	-1	-1	0
x_2	0	1	0	-1	-1
x_3	-1	0	1	0	-1
x_4	-1	-1	0	1	0
x_5	0	-1	-1	0	1

the point $(-1 + \varepsilon, 1 + \varepsilon)$ for some small irrational $\varepsilon > 0$, which lies in the chamber $\langle v_5, v_1 \rangle$. Then the five expansions of the cluster variables are shown as in Fig. 4, and these five terms generate the coordinate ring $\mathbb{C}[U]$.

For any $a, b \in \mathbb{Z}_{\geq 0}$ now consider the point $m = av_i + bv_{i+1}$ in the chamber $\langle v_i, v_{i+1} \rangle$. Since any broken line that leaves a chamber of \mathcal{D} can never return to it (cf. [12, Example 3.7]), it is easy to see that there is only one broken line for m that starts at a point q very near to m , namely the straight line that leaves q in the direction of m . Thus if we choose to expand the theta function ϑ_m by counting broken lines starting at q we obtain $\vartheta_m = \vartheta_i^a \vartheta_{i+1}^b$. This completely determines all of the theta functions associated to the points of $M_U(\mathbb{Z})$.

3.3.4. The intersection pairing Since the mirror of U constructed from \mathcal{D} is isomorphic to U , it follows that the tropicalisation N_U is self-dual, i.e. that $N_U \cong M_U$. The duality between the two affine manifolds N_U and M_U is given by extending the intersection pairing

$$\langle \cdot, \cdot \rangle : N_U(\mathbb{Z}) \times M_U(\mathbb{Z}) \rightarrow \mathbb{Z} \quad \langle n, m \rangle := v_{D_n}(\vartheta_m)$$

to an intersection pairing $\langle \cdot, \cdot \rangle : N_U \times M_U \rightarrow \mathbb{R}$ which can be calculated \mathbb{R} -linearly in each cone of the fan \mathcal{F} . Given that, as a rational function on X , the divisor of x_i is

$$\text{div } x_i = E_i + D_i - D_{i-2} - D_{i+2},$$

the pairing $N_U \times M_U \rightarrow \mathbb{R}$ can be determined by Table 1.

For example, we can now compute the five halfspaces $(x_i)^{\geq -1} \subset N_U$, which are shown in Fig. 5. Equivalently, exactly the same diagrams show the five halfspaces $(D_i)^{\geq -1} \subset M_U$.

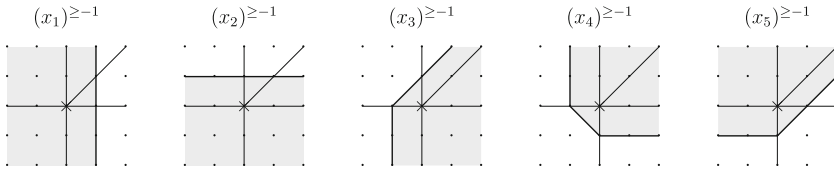


Fig. 5. The halfspaces $(x_i) \geq -1 \subset N_U$ for $i \in \mathbb{Z}/5\mathbb{Z}$

3.4. Applications to mirror symmetry

3.4.1. Reflexive polygons in N_U Now that we have built the spaces N_U and M_U as integral affine manifolds with singularities and their dual intersection pairing $\langle \cdot, \cdot \rangle: N_U \times M_U \rightarrow \mathbb{R}$, we can use them to construct examples of del Pezzo pairs and their mirror Landau–Ginzburg models, as in Sect. 2.4.3.

Theorem 3.2. *Up to automorphism there are 23 reflexive polygons in N_U , which are displayed in Fig. 6. For each reflexive polytope P , the Landau–Ginzburg model $w_Q: U \rightarrow \mathbb{C}$ obtained by labelling $Q = P^*$ with binomial edge coefficients has the right period to be a mirror to the del Pezzo pair (X_P, D_P) (where the del Pezzo surface of degree 8 represented by the unique polygon with eight vertices is \mathbb{F}_1).*

Proof. The classification of reflexive polygons in N_U proceeds in an equivalent manner to the classification of reflexive polygons in the ordinary toric setting. Beginning from any one such polygon, such as the polygon P of Example 3.3, we can add or remove vertices corresponding to blowing up or blowing down (-1) -curves in the boundary of the associated Looijenga pair (X_P, D_P) . Disregarding polygons with nonzero interior lattice points produces the 23 examples of Fig. 6.

To verify that the potential w_Q has the right period to be mirror to (X_P, D_P) , we can restrict to the cluster torus $\mathbb{T}_{12} \subset U$ to get a Laurent polynomial $w_0 := w_Q|_{\mathbb{T}_{12}} \in \mathbb{C}[x_1^{\pm 1}, x_2^{\pm 1}]$. The only difference between the Landau–Ginzburg model (U, w_Q) and the toric Landau–Ginzburg model (\mathbb{T}_{12}, w_0) is that we have extended the domain of definition of w_0 along the two exceptional curves of $U \setminus \mathbb{T}_{12}$. It is now just a case of verifying that w_0 is mutation equivalent to a known Laurent polynomial mirror to X_Q (see [1, Figure 1]). □

If $d(P)$ denotes the number of boundary points of a reflexive polygon $P \subset N_U$, then for a dual pair of reflexive polygons we have $d(P) + d(P^*) = 10$. This is in contrast to the usual formula $d(P) + d(P^*) = 12$ that holds in the ordinary toric setting, and corresponds to the fact that we have made two nontoric blowups in the boundary.

3.4.2. Examples We illustrate Theorem 3.2 with a few examples.

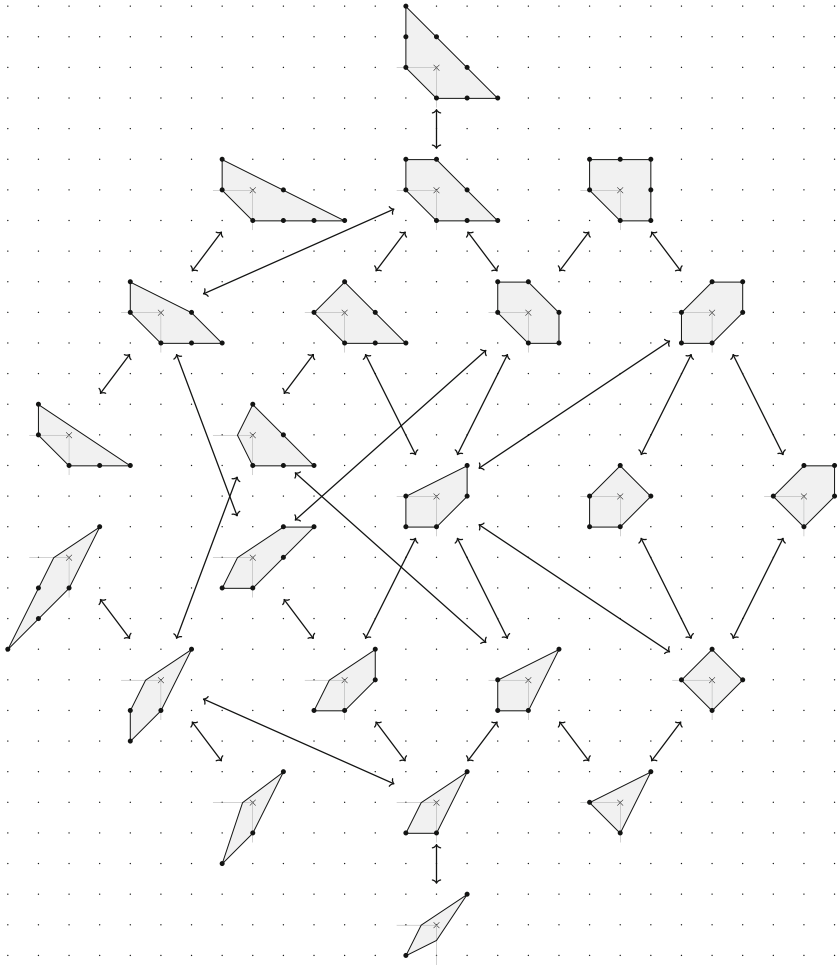
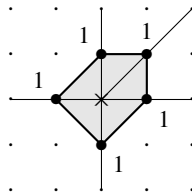


Fig. 6. Representatives for the 23 classes of reflexive polygons in N_U . The gray lines indicate the two rays along which we bend the affine structure of N_U and the arrows between polygons denote the addition or removal of a vertex. Since N_U is isomorphic to its dual space M_U , given a polygon $P \subset N_U$ we can identify the dual polygon $P^* \subset M_U$ with a polygon in N_U . Duality between these reflexive polygons is then given by top-to-bottom reflection in the diagram. In particular there are three self-dual pentagons in the central row

Example 3.3. Suppose we take the standard projective compactification (X, D) of U , which corresponds to the pair (X_P, D_P) where $P = P^*$ is the self-dual polygon



which, according to Remark 2.14, has been labelled with binomial edge coefficients. Note that P is cut out by the five halfspaces of Fig. 5. Let $w = w_P$ be the potential on the mirror Landau–Ginzburg model $w : U \rightarrow \mathbb{C}$, which is given by

$$w = x_1 + x_2 + x_3 + x_4 + x_5.$$

This is a σ_2 -invariant function, and we note that this has a nice alternative representation as $w+3 = x_1x_2x_3x_4x_5$, corresponding to the fact that the fibre $w^{-1}(-3) \subset U$ breaks up as the union of the five interior (-1) -curves $E = \bigcup_{i=1}^5 E_i$.

The period $\pi_w(t)$ By restricting w to the cluster torus chart \mathbb{T}_{12} (i.e. expanding it as a Laurent polynomial in terms of x_1, x_2), we can compute the period $\pi_w(t)$ which we see to be equal to the regularised quantum period for dP_5 . The first few terms are given by

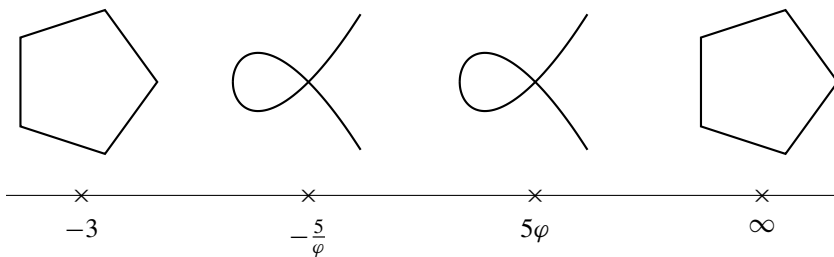
$$\pi_w(t) = 1 + 10t^2 + 30t^3 + 270t^4 + 1560t^5 + 11350t^6 + 77700t^7 + \dots$$

Alternatively, we can compute the period of the shifted potential $w + 3$, which is given by the change of variables $\pi_{w+3}(t) = \frac{1}{1-3t}\pi_w\left(\frac{t}{1-3t}\right)$. The series is

$$\pi_{w+3}(t) = 1 + 3t + 19t^2 + 147t^3 + 1251t^4 + 11253t^5 + 104959t^6 + \dots$$

which can be recognised as one of the famous Apéry series $\pi_{w+3}(t) = \sum_{n=0}^{\infty} \sum_{k=0}^n \binom{n}{k}^2 \binom{n+k}{k} t^n$ and is well-known as a period for the del Pezzo surface of degree 5.

The elliptic fibration After extending to a birational map $w : X \dashrightarrow \mathbb{P}^1$, the fibres of w belong to the anticanonical pencil $|D, E| \subset |-K_X|$ with baselocus given by the five points $D_i \cap E_i \in X$. Blowing up these five points $\phi : \tilde{X} \rightarrow X$ resolves w into an elliptic fibration $\tilde{w} = w \circ \phi : \tilde{X} \rightarrow \mathbb{P}^1$, which appears in Beauville’s classification of rational elliptic surfaces with four singular fibres [4]. There are two I_5 fibres over ∞ and -3 , corresponding to D and E respectively, and two further I_1 fibres over the values $-\frac{5}{\varphi}$ and 5φ , where $\varphi = \frac{1+\sqrt{5}}{2}$ is the golden ratio.

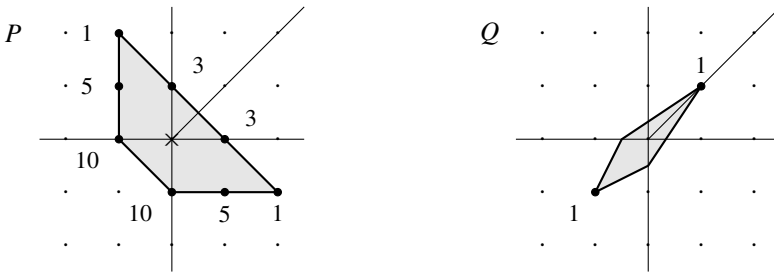


The Landau–Ginzburg model $w : U \rightarrow \mathbb{C}$ is obtained from this elliptic fibration \tilde{w} by deleting the fibre at ∞ and five horizontal sections given by the five ϕ -exceptional curves. In terms of mirror symmetry, the significance of the five deleted sections is due to the fact that the anticanonical divisor $D \subset X$ has five corners [20, Remark 2.1]. Changing the choice of boundary divisor by smoothing a corner

of D corresponds to extending w along one of the missing horizontal sections, so the Landau–Ginzburg model obtained by extending w to $\tilde{X} \setminus \tilde{w}^{-1}(\infty)$ is mirror to a del Pezzo surface of degree 5 with a smooth anticanonical divisor, as expected [3].

The fibration \tilde{w} has some very interesting arithmetic properties. The five ϕ -exceptional curves of \tilde{w} are permuted by the $\mathbb{Z}/5\mathbb{Z}$ -symmetry. For each smooth fibre \tilde{X}_t these sections give rise to the orbit of a rational 5-torsion point under translation. Moreover, the monodromy action on $H^1(\tilde{X}_t, \mathbb{Z}) \cong \mathbb{Z}^2$ around the four singular fibres generates the congruence subgroup $\Gamma_1(5) \subset \mathrm{SL}(2, \mathbb{Z})$, as shown in [5].

Example 3.4. To give a slightly more exotic example, consider the following polygon $P \subset N_U$ and its dual $Q = P^* \subset M_U$, which have also been labelled with binomial edge coefficients.



Note that both P and Q are both bigons; they each have precisely two vertices when considered in the affine structure of N_U or M_U .

Graded ring calculation for (X_Q, D_Q) Consider the theta functions $\vartheta_1, \dots, \vartheta_4$ corresponding to the lattice points $(-1, -1), (1, 1) \in Q$ and $(-1, 0), (0, -1) \in 2Q$ respectively. In terms of the basis of theta functions of $\mathbb{C}[U]$, these are

$$\vartheta_1 = x_1x_2, \quad \vartheta_2 = x_4, \quad \vartheta_3 = x_1, \quad \vartheta_4 = x_2$$

and, after homogenising, they can be used to give a presentation of the graded ring $R_Q = \mathbb{C}[\vartheta_0, \vartheta_1, \vartheta_2, \vartheta_3, \vartheta_4]/I$ with generators in degrees 1, 1, 1, 2, 2 respectively. The ideal of equations I defining R_Q is generated by two relations

$$\vartheta_0^3\vartheta_1 = \vartheta_3\vartheta_4 \quad \text{and} \quad \vartheta_1\vartheta_2 = \vartheta_0^2 + \vartheta_3 + \vartheta_4.$$

Using the second equation to eliminate ϑ_4 , we get a quartic hypersurface

$$X_Q \cong \mathbb{V} \left(\vartheta_1\vartheta_2\vartheta_3 - \vartheta_0^3\vartheta_1 - \vartheta_0^2\vartheta_3 - \vartheta_3^2 \right) \subset \mathbb{P}(1, 1, 1, 2)_{\vartheta_0, \vartheta_1, \vartheta_2, \vartheta_3}.$$

As may be expected from the spanning fan of $P \subset N_U$, this defines a singular del Pezzo surface of degree 2, with an A_2 singularity at the coordinate point $P_1 = (0 : 1 : 0 : 0)$ and an A_4 singularity at the coordinate point $P_2 = (0 : 0 : 1 : 0)$. The boundary divisor $D_Q = \mathbb{V}(\vartheta_0)$ has two components

$$D_1 = \mathbb{V}(\vartheta_0, \vartheta_3), \quad D_2 = \mathbb{V}(\vartheta_0, \vartheta_1\vartheta_2 - \vartheta_3)$$

which meet at the two singular points P_1, P_2 .

The Landau–Ginzburg model $w_P : U \rightarrow \mathbb{C}$ We form the Landau–Ginzburg potential

$$w_P = x_2 x_3^2 + 3x_3 + 3x_5 + x_5^2 x_1 + 5x_5 x_1 + 10x_1 + 10x_2 + 5x_2 x_3$$

obtained by considering binomial edge coefficients on P . By restricting to the torus chart $\mathbb{T}_{12} \subset U$ we obtain a Laurent polynomial, which satisfies the following identity

$$(w_P + 12) |_{\mathbb{T}_{12}} = \frac{(1 + x_1 + x_2)^2 (x_1 + x_2)^3}{x_1^2 x_2^2}.$$

By Sect. 2.4.2, the n th coefficient α_n of the period $\pi_{w+12}(t) = \sum_{n \geq 0} \alpha_n t^n$ is equal to the coefficient of $x_1^{2n} x_2^{2n}$ in

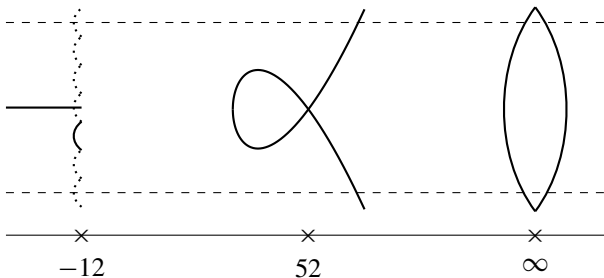
$$(1 + x_1 + x_2)^{2n} (x_1 + x_2)^{3n} = \sum_{k=0}^{2n} \binom{2n}{k} (x_1 + x_2)^{3n+k},$$

where the righthand side was obtained by expanding the first bracket by using the binomial formula, treating $1 + x_1 + x_2$ as the sum of 1 and $x_1 + x_2$. The term $x_1^{2n} x_2^{2n}$ can only appear in the righthand side if $k = n$, and then we easily see that

$$\alpha_n = \binom{2n}{n} \binom{4n}{2n} \implies \pi_{w_P+12}(t) = \sum_{k \geq 0} \frac{(4n)!}{n!n!(2n)!} t^n.$$

This function $\pi_{w_P+12}(t)$ is equal to the *regularised I-function* $\widehat{I}_{X_4}(t)$ for a hypersurface $X_4 \subset \mathbb{P}(1, 1, 1, 2)$, and it is known to be a shift of the regularised quantum period $\widehat{G}_{X_4}(t)$ of X_4 [8, Proposition D.9]. In order to recover $\widehat{G}_{X_4}(t)$ from $\widehat{I}_{X_4}(t)$, the appropriate shift is by the unique constant term required to kill the coefficient α_1 of $\widehat{I}_{X_4}(t)$. Since $\alpha_1 = \binom{2}{1} \binom{4}{2} = 12$ we see that $\pi_{w_P}(t) = \widehat{G}_{X_4}(t)$.

This shows that w_P has the right period to be mirror to X_Q , but, more precisely, we expect that the particular Landau–Ginzburg model that we have constructed is actually a mirror to the (singular) del Pezzo surface X_Q with its boundary divisor D_Q . Note that w_P has a reducible fibre $w_P^{-1}(-12)$ with two disjoint components; one component of multiplicity 2 and one of multiplicity 3. After extending w_P to the dual compactification $w_P : X_P \dashrightarrow \mathbb{P}^1$, blowing up two basepoints and then resolving singularities, we obtain an extremal rational elliptic fibration with three singular fibres of type I_1, I_2 and \widetilde{E}_7 over the points $52, \infty$ and -12 respectively.



The two components of multiplicity 2 and 3 are given by the two solid lines in the \tilde{E}_7 fibre, shown in the diagram above. The surface U is obtained by deleting the two horizontal (-1) -curves, as well as the six dotted (-2) -curves in the \tilde{E}_7 fibre. We saw above that the presence of an ordinary node in the boundary divisor $D_Q \subset X_Q$ corresponds to the deletion of a horizontal (-1) -curve in the mirror to (X_Q, D_Q) . This example suggests that the presence of an A_k singularity at a node corresponds to the deletion of a chain of $k + 1$ rational curves of self-intersection $(-1, -2, \dots, -2)$.

Example 3.5. One can do the computations of Example 3.4 with the roles of P and Q reversed. The graded ring R_P is the homogeneous coordinate ring of a smooth surface $X_P \subset \mathbb{P}^8$, which is an anticanonically polarised \mathbb{F}_1 . The boundary divisor $D_P = D_1 \cup D_2$ is the union of two smooth rational curves of self-intersection $D_1^2 = 1$ and $D_2^2 = 3$. By restricting to $\mathbb{T}_{12} \subset U$ we see that the Landau–Ginzburg potential satisfies $w_Q|_{\mathbb{T}_{12}} = x_1x_2 + \frac{1}{x_1} + \frac{1}{x_2} + \frac{1}{x_1x_2}$ which is a mirror Laurent polynomial for \mathbb{F}^1 .

4. Dimension 3: the Fano 3-fold V_{12}

We now describe a parallel story in the 3-dimensional setting which generalises

1. the cluster structure on U the affine del Pezzo surface of degree 5,
2. the fibration on the affine cone over $\text{Gr}(2, 5)$ by such surfaces,
3. the self-dual integral affine manifold with singularities N_U obtained by tropicalising U ,
4. the Borisov–Batyrev style mirror symmetry constructions of Sect. 3.4.

Indeed, the corresponding actors will be the orthogonal Grassmannian $\text{OGr}(5, 10)$ and the Fano 3-fold V_{12} . We will begin by generalising the second statement by giving a description of $\text{OGr}(5, 10)$ which leads to a homogenisation of the 3-dimensional Lyness recurrence (LR₃).

4.1. The orthogonal Grassmannian $\text{OGr}(5, 10)$

4.1.1. $\text{OGr}(5, 10)$ as a homogeneous variety The orthogonal Grassmannian $\text{OGr}(5, 10)$ is one of the two isomorphic irreducible components in the space of 5-planes $\mathbb{C}^5 \subset \mathbb{C}^{10}$ which are isotropic with respect to a given quadratic form. It is the homogeneous variety for the group $\text{SO}(10)$ of type D_5 with a ‘half-spinor embedding’ $\text{OGr}(5, 10) \subset \mathbb{P}(S^+)$, where S^+ is one half of the spin representation $S^+ \oplus S^-$ of $\text{SO}(10)$. Given the symmetry broken by choosing S^+ over S^- , it is perhaps better to think of the isomorphic Grassmannian $\text{OGr}(4, 9) \cong \text{OGr}(5, 10)$ instead. This is a homogeneous variety for the group $\text{SO}(9)$ of type B_4 , with spinor embedding $\text{OGr}(4, 9) \subset \mathbb{P}(S)$ corresponding to the (irreducible) spin representation $S = \bigoplus_{i=0}^4 \wedge^i \mathbb{C}^4$ of $\text{SO}(9)$.



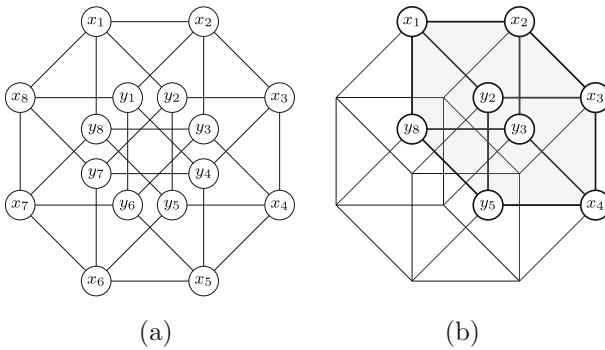


Fig. 7. a The sixteen spinor variables labelling the 4-cube C . **b** The face of C which corresponds to the equation $x_1x_4 = x_2y_5 + x_3y_8 + y_2y_3$

The representation S is 16-dimensional with weights $\frac{1}{2}(\pm 1, \pm 1, \pm 1, \pm 1)$, which are the vertices of a 4-dimensional cube C in the weight lattice for B_4 . The Weyl group $W(B_4)$ acts as the full symmetry group of C and a Coxeter element in $W(B_4)$ acts on C as a rotation of order 8. Taking the orthogonal projection onto the Coxeter plane (shown in Fig. 7a) we see this 8-fold rotational symmetry of C which splits the vertices into two groups of size 8.

4.1.2. The equations of $OGr(5, 10)$ Let $R = \mathbb{C}[S]$ and name the 16 spinor variables $x_1, \dots, x_8, y_1, \dots, y_8 \in R$, indexed by $\mathbb{Z}/8\mathbb{Z}$, according to the labels in Fig. 7a. The corresponding vertices of C are represented by the columns of the following matrix (where the minus signs in front of y_3 and y_7 are only chosen to make the equations displayed below more beautiful).

x_1	x_2	x_3	x_4	x_5	x_6	x_7	x_8	y_1	y_2	$-y_3$	y_4	y_5	y_6	$-y_7$	y_8
+	-	-	-	+	+	+	+	-	+	-	-	+	-	+	+
+	+	-	-	-	+	+	+	+	-	+	-	-	+	-	+
+	+	+	-	-	-	-	+	+	+	-	+	-	-	+	-
+	+	+	+	-	-	-	-	-	+	+	-	+	-	-	+

The ten quadratic equations defining $OGr(5, 10)$ are now obtained by swapping minus signs in columns that differ in three or more places. For example,

$$\begin{pmatrix} + \\ + \\ + \\ + \end{pmatrix} \begin{pmatrix} + \\ - \\ - \\ - \end{pmatrix} = \begin{pmatrix} + \\ + \\ + \\ - \end{pmatrix} \begin{pmatrix} + \\ - \\ - \\ + \end{pmatrix} - \begin{pmatrix} + \\ - \\ + \\ - \end{pmatrix} \begin{pmatrix} + \\ + \\ - \\ + \end{pmatrix} + \begin{pmatrix} + \\ + \\ - \\ - \end{pmatrix} \begin{pmatrix} + \\ - \\ + \\ + \end{pmatrix}$$

corresponds to the equation $x_1x_6 = x_8y_5 + y_7y_8 + x_7y_2$. The full ideal I defining $OGr(5, 10)$ is given by

$$\begin{aligned} x_1x_4 &= x_2y_5 + x_3y_8 + y_2y_3 \\ x_5x_8 &= x_6y_1 + x_7y_4 + y_6y_7 \\ x_1x_5 - x_3x_7 &= y_1y_5 - y_3y_7 \end{aligned}$$

$$\begin{aligned}
 x_2x_5 &= x_3y_6 + x_4y_1 + y_3y_4 \\
 x_6x_1 &= x_7y_2 + x_8y_5 + y_7y_8 \\
 x_2x_6 - x_4x_8 &= y_2y_6 - y_4y_8 \\
 x_3x_6 &= x_4y_7 + x_5y_2 + y_4y_5 \\
 x_7x_2 &= x_8y_3 + x_1y_6 + y_8y_1 \\
 x_4x_7 &= x_5y_8 + x_6y_3 + y_5y_6 \\
 x_8x_3 &= x_1y_4 + x_2y_7 + y_1y_2
 \end{aligned}$$

where the first two columns give the eight periodic relations

$$x_i x_{i+3} = x_{i+1} y_{i+4} + x_{i+2} y_{i-1} + y_{i+1} y_{i+2} \quad i \in \mathbb{Z}/8\mathbb{Z}$$

which are a homogenisation of (LR₃) by the variables y_1, \dots, y_8 . The binomials appearing in these eight equations correspond to the antipodal vertices in the eight 3-cube faces of C , as shown in Fig. 7b. The last two equations are implied from the first eight and correspond to the two orthopteres (4-dimensional octahedra) inscribed on the two bipartite decompositions on the set of vertices of C .

The affine cone \mathcal{U} We let $\mathcal{U} = \text{Spec}(R/I) \subset \mathbb{A}^{16}$ be the affine variety defined by these equations, i.e. the affine cone over $\text{OGr}(5, 10)$. Note that there is a map $i: \mathcal{U} \rightarrow \mathcal{U}$ with $i(x_i) = -y_{3i}$ and $i(y_i) = x_{3i+4}$, which switches the role of the x variables and the y variables. Therefore, after setting $x_i = -1$ for all i we see that $(y_{3i}: i \in \mathbb{Z}/8\mathbb{Z})$ is also a solution to the Lyness recurrence (LR₃).

Anticanonical class The ideal I is a Gorenstein ideal of codimension 5 and has minimal resolution

$$R \leftarrow R(-2)^{\oplus 10} \leftarrow R(-3)^{\oplus 16} \leftarrow R(-5)^{\oplus 16} \leftarrow R(-6)^{\oplus 10} \leftarrow R(-8) \leftarrow 0.$$

From the last module we can read off the adjunction number for $\mathcal{U} \subset \mathbb{A}^{16}$, giving $-K_{\mathcal{U}} = \mathcal{O}_{\mathbb{A}^{16}}(16 - 8)|_{\mathcal{U}} = \mathcal{O}_{\mathcal{U}}(8)$. In particular, if we let $\mathcal{D}_i = \mathbb{V}(y_i)$ and $\mathcal{E}_i = \mathbb{V}(x_i)$ for $i = 1, \dots, 8$, then both $\mathcal{D} = \bigcup_{i=1}^8 \mathcal{D}_i$ and $\mathcal{E} = \bigcup_{i=1}^8 \mathcal{E}_i$ define anticanonical divisors in \mathcal{U} .

4.1.3. A fibration of \mathcal{U} by affine Fano 3-folds Consider the projection $p: \mathcal{U} \rightarrow \mathbb{A}_{y_1, \dots, y_8}^8$. The fibres of p are a flat family of affine Gorenstein 3-folds which spreads out the components of \mathcal{D} above the coordinate strata of \mathbb{A}^8 .

The central fibre U_0 The central fibre $U_0 := p^{-1}(0)$ is given by the common intersection of all components of $\mathcal{D} \subset \mathcal{U}$. It breaks up a reducible affine toric 3-fold with ten components:

$$\bigcap_{i=1}^8 \mathcal{D}_i = \mathbb{V}(y_1, \dots, y_8) = \bigcup_{i=1}^8 \mathbb{A}_{x_{i-1}, x_i, x_{i+1}}^3 \cup Q_{1357} \cup Q_{2468}$$

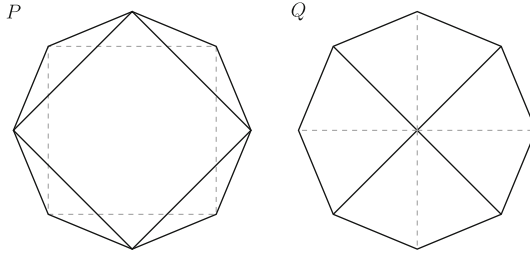


Fig. 8. The polytope P and the dual polytope $Q = P^*$

where $Q_{1357} = \mathbb{V}(x_1x_5 - x_3x_7) \subset \mathbb{A}_{x_1,x_3,x_5,x_7}^4$ and $Q_{2468} = \mathbb{V}(x_2x_6 - x_4x_8) \subset \mathbb{A}_{x_2,x_4,x_6,x_8}^4$ are both isomorphic to the cone over the Segre embedding of $\mathbb{P}^1 \times \mathbb{P}^1$. Therefore U_0 looks like the cone over a reducible toric surface

$$D_P := D_{123} \cup D_{234} \cup \dots \cup D_{812} \cup D_{1357} \cup D_{2468},$$

with ten components $D_{1357} = \mathbb{P}(Q_{1357})$, $D_{2468} = \mathbb{P}(Q_{2468})$ and $D_{123} = \mathbb{P}_{x_1,x_2,x_3}^2$, etc. These components intersect along their toric boundary strata like the polytope P of Fig. 8.

The general fibre $U_{\lambda,\mu}$ We now look at a general fibre of this fibration $U_y = p^{-1}(y)$ where $y = (y_1, \dots, y_8) \in (\mathbb{C}^\times)^8$. We can rescale the coordinates on U_y by

$$(x_1, \dots, x_8) \mapsto \left(\frac{y_1y_2}{y_4}x_1, \frac{y_1y_2}{y_7}x_2, \frac{y_2y_3}{y_8}x_3, \frac{y_4y_5}{y_7}x_4, \frac{y_4y_5}{y_2}x_5, \frac{y_4y_5y_8}{y_2y_3}x_6, \frac{y_7y_8}{y_2}x_7, \frac{y_8y_1}{y_3}x_8 \right)$$

to find that $U_y \cong U_{\lambda,\mu}$, for an affine 3-fold $U_{\lambda,\mu} \subset \mathbb{A}_{x_1,\dots,x_8}^8$ depending on two parameters $\lambda = \frac{y_3y_7}{y_1y_5}$ and $\mu = \frac{y_2y_6}{y_4y_8}$ with $\lambda, \mu \in \mathbb{C}^\times$. The equations defining $U_{\lambda,\mu}$ become:

$$\begin{aligned} x_1x_4 &= x_2 + \lambda x_3 + \lambda & x_5x_8 &= x_6 + \lambda x_7 + \lambda\mu & x_1x_5 - \lambda x_3x_7 &= 1 - \lambda \\ x_2x_5 &= \lambda\mu x_3 + x_4 + \lambda & x_6x_1 &= \lambda x_7 + x_8 + \lambda & x_2x_6 - x_4x_8 &= \lambda\mu - \lambda \\ x_3x_6 &= x_4 + x_5 + 1 & x_7x_2 &= x_8 + \mu x_1 + 1 \\ x_4x_7 &= x_5 + x_6 + \mu & x_8x_3 &= x_1 + x_2 + 1 \end{aligned}$$

Thus the fibres of p are isomorphic over the intersection of two quadrics in the base given by $\mathbb{V}(\lambda y_1y_5 - y_3y_7, y_2y_6 - \mu y_4y_8) \cap (\mathbb{C}^\times)^8$.

Lemma 4.1. *The projective closure $X_{\lambda,\mu} := \overline{U}_{\lambda,\mu} \subset \mathbb{P}^8$ has boundary divisor $D_{\lambda,\mu}$ isomorphic to D_P , and $X_{\lambda,\mu}$ has 16 ordinary (non- \mathbb{Q} -factorial) nodal singularities along $D_{\lambda,\mu}$, given by the 8 coordinate points P_{x_i} and the 8 points:*

$$\begin{aligned} (1 : -1) \in \mathbb{P}_{x_1,x_2}^1, & \quad (\lambda : -1) \in \mathbb{P}_{x_2,x_3}^1, & \quad (1 : -\lambda\mu) \in \mathbb{P}_{x_3,x_4}^1, & \quad (1 : -1) \in \mathbb{P}_{x_4,x_5}^1, \\ (1 : -1) \in \mathbb{P}_{x_5,x_6}^1, & \quad (\lambda : -1) \in \mathbb{P}_{x_6,x_7}^1, & \quad (1 : -\lambda) \in \mathbb{P}_{x_7,x_8}^1, & \quad (\mu : -1) \in \mathbb{P}_{x_8,x_1}^1. \end{aligned}$$

Moreover, the interior $U_{\lambda,\mu}$

1. is smooth if both $\lambda, \mu \neq 1$,
2. acquires one node if either $\lambda = 1$ or $\mu = 1$,
3. acquires two nodes if both $\lambda = \mu = 1$.

Proof. If $\mu = 1$ then the point $(-1, 0, -1, 0, -1, 0, -1, 0)$ belongs to $U_{\lambda,1}$ and we can eliminate the variables x_1, x_3, x_5, x_7 in a neighbourhood of this point to find an ordinary nodal singularity with local equation $(x_2x_6 - x_4x_8 = 0) \subset \mathbb{A}_{x_2,x_4,x_6,x_8}^4$. Similarly if $\lambda = 1$ the point $(0, -1, 0, -1, 0, -1, 0, -1)$ becomes a node of $U_{1,\mu}$. If both $\lambda = \mu = 1$ then this gives nodes at two distinct points of $U_{1,1}$. Smoothness elsewhere and the singular locus along $D_{\lambda,\mu}$ can be checked by computer algebra, e.g. Macaulay2. \square

4.1.4. Mirror interpretation of the family \mathcal{U} We saw in Remark 3.1 that the fibration we defined in Sect. 3.2 was not quite the same as the mirror family for (X, D) , the del Pezzo surface of degree 5, constructed by Gross et al. [12], since their mirror construction produces a family over $\text{Spec } \mathbb{C}[\overline{\text{NE}}(X)]$, rather than \mathbb{A}^5 . In a similar vein, the referee of this paper suggested the following more conceptual mirror description of our 3-dimensional family \mathcal{U} , using the geometry of $U_{1,1}$ that we work out in the rest of this section.

Following Proposition 4.15, there is a compactification (X_Q, D_Q) of the special fibre $U_{1,1}$ whose boundary divisor D_Q consists of eight copies of $\mathbb{P}^1 \times \mathbb{P}^1$ intersecting like the polytope Q . By blowing up the non-Cartier interior divisors of X_Q in some order, we can make a small partial resolution $\psi: \tilde{X}_Q \rightarrow X_Q$ that resolves 10 of the 12 nodes of X_Q but does not change the intersection complex of \tilde{D}_Q (and in particular, leaves the two nodes at the two 4-valent vertices of Q intact). The intrinsic mirror symmetry construction of Gross and Siebert [15] then produces a mirror family $p': \mathcal{U}' \rightarrow B'$ over the base $B' := \text{Spec } \mathbb{C}[\text{Nef}(\tilde{X}_Q)]$ with the same central fibre U_0 as our family \mathcal{U} .

This mirror family is equivariant for the action of the torus \mathbb{T} on B' , where $\mathbb{T} := \mathbb{T}_{\tilde{D}_Q} \cap \text{Pic } \tilde{X}_Q$ and $\mathbb{T}_{\tilde{D}_Q}$ is the torus of rank 8 generated by the irreducible components of \tilde{D}_Q . In this case \mathbb{T} has rank 6, since the coefficients of a Cartier divisor supported on D_Q must satisfy two linear conditions imposed by the two nodes. From the description of \tilde{X}_Q as the blowup of a toric variety (cf. Proposition 4.2) one can compute that $\text{Pic } \tilde{X}_Q$ has rank 8, and thus $\text{Pic } U_{1,1} \cong \text{Pic } \tilde{X}_Q / \mathbb{T}$ is a lattice of rank 2, confirming that the fibres of the mirror family \mathcal{U}' depend on two deformation parameters λ and μ . These two deformation parameters correspond to the two ψ -exceptional $\mathcal{O}(-1, -1)$ -curves over the two interior nodes of $U_{1,1}$ on one side of the mirror, and the two vanishing Lagrangian spheres S^3 in the smoothing of $U_{1,1}$ on the other side.

As in Remark 3.1, our family \mathcal{U} should now rather be viewed as an extension of this mirror family $p': \mathcal{U}' \rightarrow B'$ to a family $p: \mathcal{U} \rightarrow \mathbb{A}^8$ defined over the base $\mathbb{A}^8 = \text{Spec } \mathbb{C}[\sigma^*]$, where $\sigma^* \supseteq \text{Nef}(\tilde{X}_Q)$ is dual to the cone $\sigma \subset A_1(\tilde{X}_Q)$ generated by the classes of 1-strata in the boundary of $(\tilde{X}_Q, \tilde{D}_Q)$. This cone is independent of the choice of small resolution ψ of X_Q , and one would expect it to be equal to the cone containing $\text{Nef}(\tilde{X}_Q)$ in the *secondary fan* of $(\tilde{X}_Q, \tilde{D}_Q)$, as defined by Hacking et al. [18].

4.2. The affine Fano-3-fold $U_{\lambda,\mu}$

We now study the affine Fano 3-fold $U_{\lambda,\mu} = X_{\lambda,\mu} \setminus D_{\lambda,\mu}$, which has a (generalised) cluster structure and is the 3-dimensional analogue of the affine del Pezzo surface considered in Sect. 3.

4.2.1. *Blowup description of $U_{\lambda,\mu}$* One way that the affine del Pezzo surface can be obtained is by blowing up one point on each of the coordinate axis in \mathbb{A}^2 and deleting the strict transform of the boundary. We now give a similar description for the 3-folds $U_{\lambda,\mu}$.

Proposition 4.2. *Let $H = \mathbb{V}(x_1x_2x_3) \subset \mathbb{A}^3$ denote the union of the coordinate hyperplanes. There is a locus $Z \subset H \subset \mathbb{A}^3$ such that $U_{\lambda,\mu} \cong \text{Bl}_Z(\mathbb{A}^3) \setminus \tilde{H}$ —i.e. the blowup of Z minus the strict transform of H . According to the cases of Lemma 4.1:*

1. if $\lambda, \mu \neq 1$ then Z consists of a conic and two lines

$$Z = \mathbb{V}(x_1, \lambda + x_2 + \lambda x_3) \cup \mathbb{V}(x_2, 1 + x_1 + x_3 + \mu x_1 x_3) \\ \cup \mathbb{V}(x_3, 1 + x_1 + x_2),$$

2. if $\lambda \neq 1, \mu = 1$ then Z consists of four lines (two lines and a reducible conic)

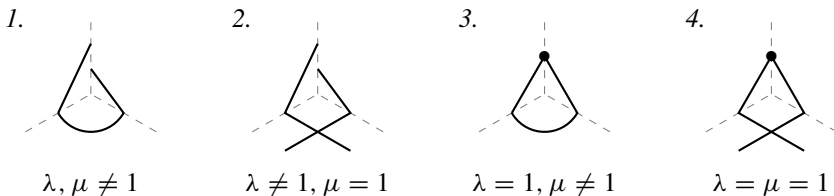
$$Z = \mathbb{V}(x_1, \lambda + x_2 + \lambda x_3) \cup \mathbb{V}(x_2, 1 + x_1) \cup \mathbb{V}(x_2, 1 + x_3) \\ \cup \mathbb{V}(x_3, 1 + x_1 + x_2),$$

3. if $\lambda = 1, \mu \neq 1$ then Z consists of a conic and two lines meeting at an embedded point

$$Z = \mathbb{V}(x_1, 1 + x_2 + x_3) \cup \mathbb{V}(x_2, 1 + x_1 + x_3 + \mu x_1 x_3) \\ \cup \mathbb{V}(x_3, 1 + x_1 + x_2) \cup \mathbb{V}(x_1, 1 + x_2, x_3),$$

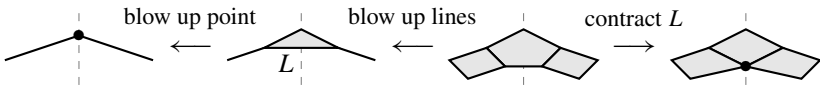
4. if $\lambda = \mu = 1$ then Z consists of a reducible conic and two lines meeting at an embedded point

$$Z = \mathbb{V}(x_1, 1 + x_2 + x_3) \cup \mathbb{V}(x_2, 1 + x_1) \cup \mathbb{V}(x_2, 1 + x_3) \\ \cup \mathbb{V}(x_3, 1 + x_1 + x_2) \cup \mathbb{V}(x_1, 1 + x_2, x_3).$$

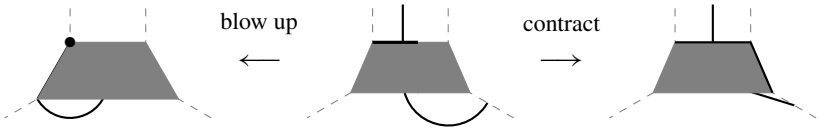


Remark 4.3. Before proving the proposition, we briefly describe the effect of the blowups we make and explain how $U_{\lambda,\mu}$ ends up with the number of nodes expected from Lemma 4.1.

1. The blowup $Bl_Z(\mathbb{A}^3)$ obtains an ordinary node in the fibre over any point $P \in Z$ contained in the intersection of two curves. If P is contained in a 1-stratum of the boundary then after the blowup the node is contained in \tilde{H} and hence does not appear in $U_{\lambda,\mu}$. However, if P is contained in the interior of a 2-stratum (as happens in cases 2. and 4.) then the node is not contained in \tilde{H} and therefore must appear in $U_{\lambda,\mu}$.
2. Blowing up an embedded point in the intersection of two lines also produces a node in the interior $U_{\lambda,\mu}$ (as happens in cases 3. and 4.). To see how, we can first blow up the embedded point with exceptional divisor E . Let $L \subset E$ be the line that passes through the strict transform of the two lines on either side. Blowing up the lines turns L into a contractible $\mathcal{O}(-1, -1)$ curve, which is contracted to an ordinary node.



3. It is interesting that cases 2. and 3. give two different constructions of varieties that should be isomorphic by exchanging the role of λ and μ . Indeed, we can send the configuration 3. to the configuration 2. by the mutating one of the two line components, e.g. we blow up the line $\mathbb{V}(x_3, 1 + x_1 + x_2)$ and then contract the strict transform of the divisor $\mathbb{V}(1 + x_1 + x_2)$ to the plane at infinity.



Proof. Consider $g: U_{\lambda,\mu} \subset \mathbb{A}^8 \rightarrow \mathbb{A}_{x_1,x_2,x_3}^3$, which is a birational projection of $U_{\lambda,\mu}$ onto its image. This image is the constructible set

$$g(U_{\lambda,\mu}) = (\mathbb{C}^\times)_{x_1,x_2,x_3}^3 \cup Z^0, \quad \text{where } Z^0 = \begin{cases} Z \setminus \mathbb{V}(x_1, x_3) & \text{if } \lambda \neq 1 \\ Z & \text{if } \lambda = 1 \end{cases}$$

and Z is as in the statement of the proposition. (In other words, if $\lambda \neq 1$ the image of $U_{\lambda,\mu}$ misses the two points of Z that lie on the x_2 -axis.) Now g restricts to an isomorphism on the open torus $(\mathbb{C}^\times)_{x_1,x_2,x_3}^3 \subset U_{\lambda,\mu}$ and we can check that the fibres over $z \in Z$ are all affine lines $g^{-1}(z) \cong \mathbb{A}^1$, unless $\lambda = 1$ and $z = (0, -1, 0)$, in which case $g^{-1}(z) \cong \mathbb{A}^2$. We can resolve the inverse map $g^{-1}: g(U_{\lambda,\mu}) \dashrightarrow U_{\lambda,\mu}$ by blowing up $Z \subset \mathbb{A}^3$, as described in Remark 4.3. \square

4.2.2. The exchange graph of $U_{\lambda,\mu}$ Recall our fibration $p: \mathcal{U} \rightarrow \mathbb{A}_{y_1,\dots,y_8}^8$, which we can think of as a family of affine 3-folds over the coefficient ring $R_y = \mathbb{C}[y_1, \dots, y_8]$. We let $\mathbb{A}_y := \mathbb{A}_{y_1,\dots,y_8}^8$ denote the base of this fibration. In the traditional language of cluster algebras, we think of the x variables as *cluster variables* on \mathcal{U} and the y variables as *frozen variables*. Moreover, we recall the two

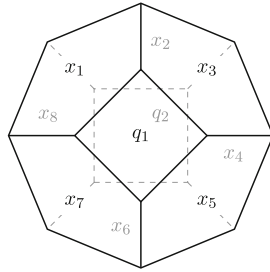


Fig. 9. The exchange graph G for the affine charts covering \mathcal{U}

quadratic terms q_1, q_2 which we introduced in Sect. 1.2.2. These are homogenised as follows:

$$q_1 := x_1x_5 - y_1y_5 = x_3x_7 - y_3y_7, \quad q_2 := x_2x_6 - y_2y_6 = x_4x_8 - y_4y_8.$$

For convenience of notation, we let $q_1 = q_3 = q_5 = q_7$ and $q_2 = q_4 = q_6 = q_8$. For reasons that will shortly become clear (see Remark 4.5), we want to add q_1 and q_2 to our list of cluster variables.

Lemma 4.4. *For any $i = 1, \dots, 8$, we have*

$$\begin{aligned} x_1, \dots, x_8, q_1, q_2 &\in R_y[x_{i-1}^{\pm 1}, x_i^{\pm 1}, x_{i+1}^{\pm 1}] \quad \text{and} \\ x_1, \dots, x_8, q_1, q_2 &\in R_y[x_i^{\pm 1}, q_i^{\pm 1}, x_{i+2}^{\pm 1}]. \end{aligned}$$

Proof. This is straightforward to check by simply expanding all of the cluster variables in the corresponding Laurent ring. \square

We let $\mathbb{T}_{i-1,i,i+1} := \text{Spec } R_y[x_{i-1}^{\pm 1}, x_i^{\pm 1}, x_{i+1}^{\pm 1}]$ and $\mathbb{T}_{i,q,i+2} = \text{Spec } R_y[x_i^{\pm 1}, q_i^{\pm 1}, x_{i+2}^{\pm 1}]$ for $i \in \mathbb{Z}/8\mathbb{Z}$. Then Lemma 4.4 shows that these give a system of 16 open affine charts in \mathcal{U} of the form $\mathbb{T} = (\mathbb{C}^\times)^3 \times \mathbb{A}_y$, which we can represent at the vertices of the exchange graph G shown in Fig. 9. The graph is the 1-skeleton of a 3-dimensional polytope and we can label the faces of this polytope so that the three faces around each vertex give the coordinates on the torus factor of each chart. The edges of G correspond to the three different types of exchange relation:

$$\begin{aligned} x_{i-1}x_{i+2} &= x_iy_{i+3} + x_{i+1}y_{i-2} + y_iy_{i+1}, \\ x_{i-2}x_{i+2} &= q_i + y_{i-2}y_{i+2}, \\ x_iq_{i-1} &= x_{i-1}x_{i+1}y_{i+4} + x_{i-1}y_{i+1}y_{i+2} + x_{i+1}y_{i-1}y_{i-2} + y_{i-1}y_iy_{i+1}. \end{aligned}$$

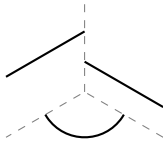
Remark 4.5. We can also now see the geometrical reason as to why we are led to include q_1 and q_2 in our list of cluster variables. In the coordinates on the fibre $U_{\lambda,\mu}$ of \mathcal{U} described above, and in the case $\lambda, \mu \neq 1$, from the blowup up description $U_{\lambda,\mu} = \text{Bl}_Z(\mathbb{A}_{x_1,x_2,x_3}^3) \setminus \tilde{H}$ of Proposition 4.2 we see that the exchange map

$$(x_1, x_2, x_3) \mapsto \left(x_2, x_3, \frac{\lambda x_2 + x_3 + \lambda}{x_1} \right),$$

is a mutation along one of the two line components of Z . Similarly, the exchange map

$$(x_1, x_2, x_3) \mapsto \left(x_1, \frac{\mu x_1 x_3 + x_1 + x_3 + 1}{x_2}, x_3 \right),$$

is a mutation along the conic component of Z . This transforms the centres along which we obtain our blowup description as follows: now $U_{\lambda, \mu} = \text{Bl}_{Z'}(\mathbb{A}_{x_1, q_1, x_3}^3) \setminus \tilde{H}'$ where $H' = \mathbb{V}(x_1 q_1 x_3)$ and $Z' \subset H'$ is the union of the following three components.



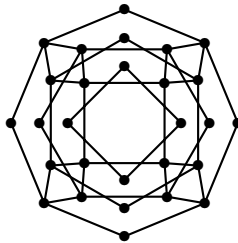
$$Z' = \bigcup \begin{cases} \mathbb{V}(x_1, \lambda q_1 + 1) \\ \mathbb{V}(q_1, \mu x_1 x_3 + x_1 + x_3 + 1) \\ \mathbb{V}(x_3, q_1 + 1) \end{cases}$$

From this we see that the final type of exchange map

$$(x_1, q_1, x_3) \mapsto \left(x_3, q_1, \frac{\lambda q_1 + 1}{x_1} \right),$$

is a mutation along one of the two line components of Z' . The nice surprise is that this system of torus charts and mutations forms a closed system (i.e. composing mutations around closed cycles in G gives the identity map on the corresponding torus chart).

Remark 4.6. In the cases where one or both of $\lambda, \mu = 1$ the number of centres to blow up in the locus Z increases from three to either four or five respectively. Therefore the valency of the mutation graph also increases. After a fairly involved computation explicitly tracking the centres of Z (which includes having to deal with unexpected jumps similar to those described in Sect. 2.2.3), it can be shown that the exchange graph of $U_{1, \mu}$ (or equivalently $U_{\lambda, 1}$) is 4-valent with 28 vertices. Similarly the exchange graph of $U_{1, 1}$ is 5-valent with 48 vertices. In particular, these exchange graphs are also finite. The exchange graph for the rank 5 case is a bit too complicated to draw elegantly, however the rank 4 case gives the following graph



which is the 1-skeleton of a 4-dimensional polytope. Visually, we see that it can be ‘collapsed’ onto the exchange graph G of Fig. 9.

4.2.3. *The interior divisors inside $U_{\lambda,\mu}$* We consider the following ten interior divisors of $U_{\lambda,\mu}$

$$E_i = \mathbb{V}(x_i) \text{ for } i = 1, \dots, 8 \text{ and } F_i = \mathbb{V}(q_i) \text{ for } i = 1, 2.$$

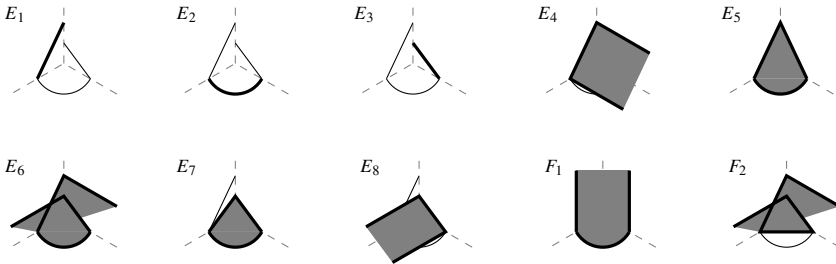
These are all the divisors that appear in the complement of one of the 16 cluster tori and are the analogue of the five interior (-1) -curves of the del Pezzo surface in Sect. 3. Because of the jump in the rank of the class group $\text{Cl}(U_{\lambda,\mu})$, something special happens to these divisors when either or both of $\lambda, \mu = 1$.

- Proposition 4.7.** 1. *If $\lambda, \mu \neq 1$, then the divisors E_i and F_i are all irreducible.*
 2. *If $\mu = 1$, the four ‘odd’ divisors E_1, E_3, E_5, E_7 break up into four overlapping irreducible components $E_{13}, E_{35}, E_{57}, E_{71}$, where $E_{13} = \mathbb{V}(x_1, x_3)$ etc. Moreover F_2 breaks into two components as $F_2 = F_{26} \cup F_{48}$, where $F_{26} = \mathbb{V}(1 + x_2, 1 + x_6)$ and $F_{48} = \mathbb{V}(1 + x_4, 1 + x_8)$.*
 3. *If $\lambda = 1$, the four ‘even’ divisors E_2, E_4, E_6, E_8 and F_1 all break into two components, with the analogous description to (2).*

In particular, if $\lambda = \mu = 1$ then all ten divisors break up into a total of twelve components.

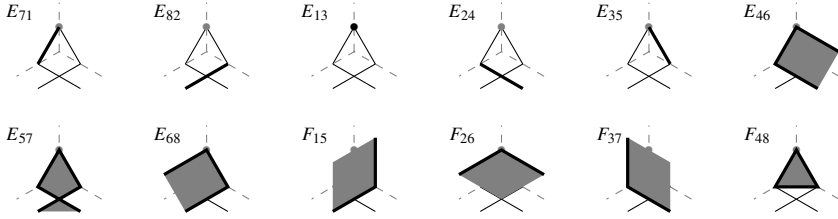
Proof. We consider the image of these divisors under the projection $g : U_{\lambda,\mu} \rightarrow \mathbb{A}^3_{x_1,x_2,x_3}$ with the discriminant locus $Z \subset \mathbb{A}^3$ as in Proposition 4.2. For $\lambda, \mu \neq 1$ we find that E_1, E_2, E_3 are the exceptional divisors over the three components of Z and the remaining divisors are given by the strict transform under g^{-1} of the following (irreducible) divisors in \mathbb{A}^3 .

$$\begin{array}{ll} E_1 : x_1 = \lambda + x_2 + \lambda x_3 = 0 & E_6 : (1 + x_1 + x_2)(\lambda + x_2 + \lambda x_3) = \lambda(1 - \mu)x_1x_3 \\ E_2 : x_2 = 1 + x_1 + x_3 + \mu x_1x_3 = 0 & E_7 : 1 + x_1 + x_2 + x_3 + \mu x_1x_3 = 0 \\ E_3 : x_3 = 1 + x_1 + x_2 = 0 & E_8 : 1 + x_1 + x_2 = 0 \\ E_4 : \lambda + x_2 + \lambda x_3 = 0 & F_1 : 1 + x_1 + x_3 + \mu x_1x_3 = 0 \\ E_5 : \lambda + \lambda x_1 + x_2 + \lambda x_3 + \lambda \mu x_3 = 0 & F_2 : (\lambda + x_2 + \lambda x_3)(1 + x_1 + x_2) = \lambda x_1x_3 \end{array}$$



If $\mu = 1$ the conic component of Z breaks into two pieces. This has the effect of breaking all the divisors E_2, E_4, E_6, E_8 and F_1 in two. If $\lambda = 1$ then the two line components of Z meet at an embedded point. This has the effect of breaking all the divisors E_1, E_3, E_5, E_7 and F_2 in two. In the most extreme case when $\lambda = \mu = 1$, the ten divisors break up into twelve components as follows.

$$\begin{array}{lll} E_{71} : x_1 = 1 + x_2 + x_3 = 0 & E_{35} : x_3 = 1 + x_1 + x_2 = 0 & F_{15} : 1 + x_1 = 0 \\ E_{82} : x_2 = 1 + x_1 = 0 & E_{46} : 1 + x_2 + x_3 = 0 & F_{26} : 1 + x_2 = 0 \\ E_{13} : x_1 = 1 + x_2 = x_3 = 0 & E_{57} : 1 + x_1 + x_2 + x_3 + x_1x_3 = 0 & F_{37} : 1 + x_3 = 0 \\ E_{24} : x_2 = 1 + x_3 = 0 & E_{68} : 1 + x_1 + x_2 = 0 & F_{48} : 1 + x_1 + x_2 + x_3 = 0 \end{array}$$



□

4.3. The tropicalisation of $U_{\lambda, \mu}$

To simplify the notation in this section we let $U = U_{\lambda, \mu}$ so that the dependence on λ, μ is now left implicit. We now want to construct the tropicalisation N_U of U (as in Sect. 2.3.1), the dual space M_U and the dual intersection pairing $\langle \cdot, \cdot \rangle : N_U \times M_U \rightarrow \mathbb{R}$.

4.3.1. The intersection pairing Recall that we have a set of ten cluster variables $\{x_1, \dots, x_8, q_1, q_2\}$ and a set of ten boundary components $\{D_{123}, \dots, D_{812}, D_{1357}, D_{2468}\}$ in the boundary divisor D of our projective compactification (X, D) of U . For any cluster monomial $\vartheta_m \in \mathbb{C}[U]$ and any boundary component D_n we let $\langle D_n, \vartheta_m \rangle := \text{ord}_{D_n}(\vartheta_m)$ denote the order of vanishing of ϑ_m along D_n . We start by computing the analogous matrix to Table 1 that we will use to define the intersection pairing $\langle \cdot, \cdot \rangle : N_U \times M_U \rightarrow \mathbb{R}$. Since this matrix is symmetric, this realises a one-to-one correspondence between the ten cluster variables $x_1, \dots, x_8, q_1, q_2$ in $\mathbb{C}[U]$ and the ten boundary divisors $D_{123}, \dots, D_{812}, D_{1357}, D_{2468}$ of (X, D) .

Proposition 4.8. *Considered as rational functions on X , the cluster variables x_1 and q_1 have divisor*

$$\begin{aligned} \text{div } x_1 &= E_1 + D_{456} - D_{781} - D_{812} - D_{123} - D_{1357} \\ \text{div } q_1 &= F_1 + D_{2468} - D_{123} - D_{345} - D_{567} - D_{781} - 2D_{1357} \end{aligned}$$

and similarly for the other cluster variables, up to the Dih_8 action. In particular, each cluster variable vanishes along a unique boundary component of (X, D) , giving a one-to-one correspondence between the ten cluster variables of U and the ten components of D . With respect to this ordering, the pairing between these cluster variables and boundary components is represented by the symmetric 10×10 matrix given in Table 2.

Proof. In terms of the homogeneous equations that define X we are required to compute $\text{div}(x_0^{-1}x_1)$ and $\text{div}(x_0^{-2}q_1)$, where $x_0 \in |\mathcal{O}_X(1)|$ is the homogenising variable. Since $\text{div } x_0 = D = D_{123} + \dots + D_{812} + D_{1357} + D_{2468}$, the first formula follows from showing that, considered as a section $x_1 \in |\mathcal{O}_X(1)|$, we have

$$\text{div } x_1 = E_1 + D_{234} + D_{345} + 2D_{456} + D_{567} + D_{678} + D_{2468}$$

and the second formula follows similarly for $q_1 \in |\mathcal{O}_X(2)|$. This now follows from an explicit calculation with the equations of X . □

Table 2. The intersection numbers $\langle D_i, x_j \rangle$ for U

	D_{456}	D_{567}	D_{678}	D_{781}	D_{812}	D_{123}	D_{234}	D_{345}	D_{2468}	D_{1357}
x_1	1	0	0	-1	-1	-1	0	0	0	-1
x_2	0	1	0	0	-1	-1	-1	0	-1	0
x_3	0	0	1	0	0	-1	-1	-1	0	-1
x_4	-1	0	0	1	0	0	-1	-1	-1	0
x_5	-1	-1	0	0	1	0	0	-1	0	-1
x_6	-1	-1	-1	0	0	1	0	0	-1	0
x_7	0	-1	-1	-1	0	0	1	0	0	-1
x_8	0	0	-1	-1	-1	0	0	1	-1	0
q_1	0	-1	0	-1	0	-1	0	-1	1	-2
q_2	-1	0	-1	0	-1	0	-1	0	-2	1

Given the correspondence in Table 2 it is now convenient to rename the boundary divisors as $D_1, \dots, D_8, D_{q_1}, D_{q_2}$ so that $D_i = D_{i+3, i+4, i+5}$ corresponds to x_i for $i \in \mathbb{Z}/8\mathbb{Z}$ and $D_{q_1} = D_{2468}$ and $D_{q_2} = D_{1357}$ correspond to q_1 and q_2 . We will use Table 2 to define a complete fan \mathcal{F} in \mathbb{R}^3 which will give us both a toric model and a scattering diagram for U .

4.3.2. A toric model for U The fan \mathcal{F} In order to tropicalise U , we must first start by choosing a cluster torus chart for U . We consider the cluster torus $j: \mathbb{T}_{1q_3} \hookrightarrow U$ with coordinates x_1, q_1, x_3 , determined by the seed $Z' \subset \mathbb{A}^3$ described in Remark 4.5. This is one mutation away from the original torus chart \mathbb{T}_{123} with coordinates x_1, x_2, x_3 , corresponding to the seed $Z \subset \mathbb{A}^3$ which we used to describe a toric model for U in Proposition 4.2. The reason for this change in the choice of seed is that the irreducible components of $Z' \subset \mathbb{A}^3$ are all smooth and disjoint (as opposed to those of Z). Thus we can obtain a description of the tropicalisation of U by blowing up Z' directly, without having to blow up any of the 1-dimensional strata of \mathbb{A}^3 .

Consider the ten primitive integral vectors $v_1, \dots, v_8, w_1, w_2 \in \mathbb{Z}^3$ corresponding to the following columns

$$\begin{array}{cccccccccc}
 v_1 & v_2 & v_3 & v_4 & v_5 & v_6 & v_7 & v_8 & w_1 & w_2 \\
 \hline
 -1 & 0 & 0 & 1 & 1 & 1 & 0 & 0 & 0 & 1 \\
 0 & 1 & 0 & 1 & 0 & 1 & 0 & 1 & -1 & 2 \\
 0 & 0 & -1 & 0 & 0 & 1 & 1 & 1 & 0 & 1
 \end{array}$$

read off as the negative of the rows corresponding to x_1, q_1, x_3 in Table 2. We can define a complete fan \mathcal{F} in \mathbb{R}^3 which has rays generated by these ten vectors and whose cones are dual to the exchange graph in Fig. 9. Thus \mathcal{F} has 16 3-dimensional cones corresponding to the 16 cluster torus charts of U and 24 2-dimensional cones corresponding to the 24 possible mutations between cluster torus charts. The fan \mathcal{F} is displayed in Fig. 10.

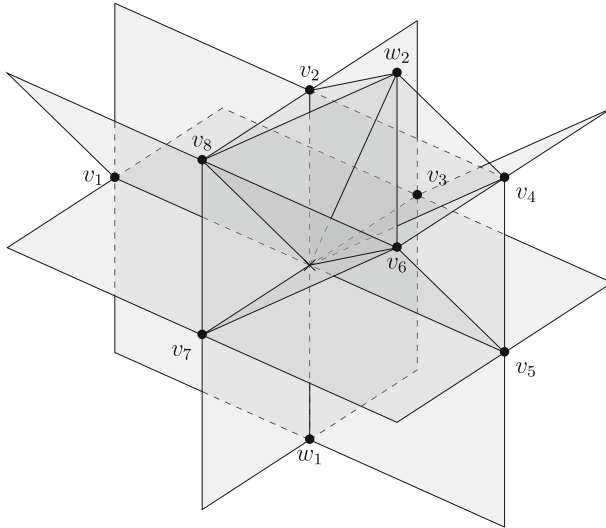


Fig. 10. The fan \mathcal{F} giving both a toric model of U , and the scattering diagram for $\mathbb{C}[U]$

The toric model for U We consider the toric variety (T, B) defined by the fan \mathcal{F} , and the locus $Z' \subset T$ determined by the seed

$$S = \{((-1, 0, 0), \lambda q_1 + 1), ((0, -1, 0), \mu x_1 x_3 + x_1 + x_3 + 1), ((0, 0, -1), q_1 + 1)\}$$

described in Remark 4.5, corresponding to the torus chart with coordinates x_1, q_1, x_3 .

Proposition 4.9. *The pair $\pi : (\tilde{X}, \tilde{D}) \rightarrow (T, B)$ obtained by blowing up $Z' \subset T$ is a toric model for U . This compactification (\tilde{X}, \tilde{D}) is a small resolution of the projective compactification (X, D) of U , and identifies the boundary components $D_1, \dots, D_8, D_{q_1}, D_{q_2}$ of D with the ten components of \tilde{D} corresponding to the vectors $v_1, \dots, v_8, w_1, w_2$ respectively.*

Proof. The proof that $\pi : (X, D) \rightarrow (T, B)$ is a toric model for U follows from extending a similar calculation to the proof of Proposition 4.2 from the toric variety \mathbb{A}^3 to the toric variety T . To see that the boundary components are identified as claimed, we can check that the identifications hold for the affine chart $\mathbb{A}_\sigma^3 = \text{Spec } \mathbb{C}[\sigma^\vee \cap M] \subset T \dashrightarrow X$ for each maximal cone $\sigma \subset \mathcal{F}$.

After blowing up the locus $Z' \subset T$ we see that the boundary divisor \tilde{D} is isomorphic to B , except for the fact that each of $\tilde{D}_1, \tilde{D}_3, \tilde{D}_5$ and \tilde{D}_7 are blown-up in two boundary points, turning these four boundary components into del Pezzo surfaces of degree 5 with an anticanonical pentagon of (-1) -curves (as in Example 3.3). The model (X, D) is now obtained from (\tilde{X}, \tilde{D}) by contracting sixteen $\mathcal{O}(-1, -1)$ -curves in the boundary (giving the sixteen nodes of Lemma 4.1). These are the eight boundary strata corresponding to the cones $\langle x_i, q_i \rangle$ for $i \in \mathbb{Z}/8\mathbb{Z}$ and eight more curves, four in each of the boundary components $\tilde{D}_1, \tilde{D}_3, \tilde{D}_5, \tilde{D}_7$, giving the eight nodes along the lines $\mathbb{P}^1_{x_i, x_{i+1}}$. These sixteen curves are indicated by the dashed lines in Fig. 11. □

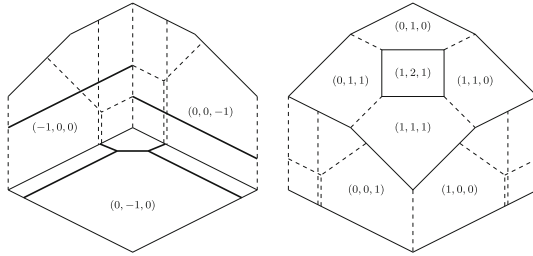


Fig. 11. A toric model $\pi: (\tilde{X}, \tilde{D}) \rightarrow (T, B)$ for U is constructed by blowing up the locus $Z' \subset B$ which is a union of three rational curves (drawn tropically with thick lines). The model (X, D) is obtained from (\tilde{X}, \tilde{D}) as a small contraction of the sixteen $\mathcal{O}(-1, -1)$ -curves (drawn tropically with dashed lines) to ordinary nodes

Remark 4.10. In Proposition 4.9 we obtained our projective compactification (\tilde{X}, \tilde{B}) of U by blowing up $Z' \subset T$. This construction uses a different seed to the seed $Z \subset \mathbb{A}^3$ appearing in Proposition 4.2, which can be used to obtain an affine partial compactification $(\text{Bl}_Z(\mathbb{A}^3), \tilde{H})$ of U . Nevertheless, (\tilde{X}, \tilde{B}) is a compactification of a small resolution of $\text{Bl}_Z(\mathbb{A}^3)$ in the following way. Note that $\text{Bl}_Z(\mathbb{A}^3)$ is singular, since the components of $Z \subset \mathbb{A}^3$ meet at points in the x_1 -axis and x_3 -axis. Consider the small resolution $\psi: (W, H_W) \rightarrow (\text{Bl}_Z(\mathbb{A}^3), \tilde{H})$, where W is obtained by first blowing up the conic component of $Z \subset \mathbb{A}^3$, and then the two lines. This (W, H_W) can be embedded inside (\tilde{X}, \tilde{B}) where the boundary components correspond to $B_{(-1,0,0)}$, $B_{(0,1,0)}$ and $B_{(0,0,-1)}$, and the two ψ -exceptional lines are the two dashed vertical lines in the relative interiors of $B_{(-1,0,0)}$ and $B_{(0,0,-1)}$, appearing in Fig. 11.

The tropicalisation N_U We can now construct N_U , the tropicalisation of U with respect to this seed, by altering the integral affine structure along the codimension 1 cones of \mathcal{F} by following the process described in Sect. 2.3.1. We arrive at the following description.

Lemma 4.11. *The integral affine structure on N_U is obtained by bending any line that passes through one of the following seven walls of \mathcal{F} :*

$$\langle v_7, v_1 \rangle, \langle v_1, v_3 \rangle, \langle v_3, v_5 \rangle, \langle v_1, w_1 \rangle, \langle v_3, w_1 \rangle, \langle v_5, w_1 \rangle, \langle v_7, w_1 \rangle.$$

If $M_{i,i+2}$ represents the bend from passing from the cone $\langle v_i, w_i, v_{i+2} \rangle$ to the cone $\langle v_i, v_{i+1}, v_{i+2} \rangle$ through the wall $\langle v_i, v_{i+2} \rangle$ for $i = 7, 1, 3$, then

$$M_{71} = \begin{pmatrix} 1 & 1 & 0 \\ 0 & 1 & 0 \\ 0 & 0 & 1 \end{pmatrix}, \quad M_{13} = \begin{pmatrix} 1 & 1 & 0 \\ 0 & 1 & 0 \\ 0 & 1 & 1 \end{pmatrix}, \quad M_{35} = \begin{pmatrix} 1 & 0 & 0 \\ 0 & 1 & 0 \\ 0 & 1 & 1 \end{pmatrix},$$

and if M_{iq} represents the bend from passing from the cone $\langle v_{i-2}, v_i, w_i \rangle$ to the cone $\langle v_i, v_{i+2}, w_i \rangle$ through the wall $\langle v_i, w_i \rangle$ for $i = 1, 3, 5, 7$, then

$$M_{1q} = \begin{pmatrix} 1 & 0 & 0 \\ -1 & 1 & 0 \\ 0 & 0 & 1 \end{pmatrix}, \quad M_{3q} = \begin{pmatrix} 1 & 0 & 0 \\ 0 & 1 & 1 \\ 0 & 0 & 1 \end{pmatrix}, \quad M_{5q} = M_{1q}^{-1}, \quad M_{7q} = M_{3q}^{-1}.$$

Table 3. Wall functions for the scattering diagram $\mathfrak{D}_{\lambda,\mu}$

Wall Function	Wall Function	Wall Function
\mathfrak{d}_{12} $1 + z_2 + z_1z_2$	\mathfrak{d}_{13} $1 + z_1 + z_3 + \mu z_1z_3$	\mathfrak{d}_{1q} $1 + z_2$
\mathfrak{d}_{23} $1 + \lambda z_2 + \lambda z_2z_3$	\mathfrak{d}_{24} $1 + z_2 + z_1z_2 + \lambda z_1z_2^2$	\mathfrak{d}_{2q} $1 + \lambda z_1z_2^2z_3$
\mathfrak{d}_{34} $1 + \lambda z_2z_3 + \lambda \mu z_1z_2z_3$	\mathfrak{d}_{35} $1 + z_1 + z_3 + \mu z_1z_3$	\mathfrak{d}_{3q} $1 + \lambda z_2$
\mathfrak{d}_{45} $1 + z_2 + z_1z_2$	\mathfrak{d}_{46} $1 + \lambda z_1z_2 + \lambda \mu z_1z_2z_3 + \lambda \mu z_1^2z_2^2z_3$	\mathfrak{d}_{4q} $1 + \lambda \mu z_1z_2^2z_3$
\mathfrak{d}_{56} $1 + z_2z_3 + \mu z_1z_2z_3$	\mathfrak{d}_{57} $1 + z_1 + z_3 + \mu z_1z_3$	\mathfrak{d}_{5q} $1 + z_2$
\mathfrak{d}_{67} $1 + \lambda z_2z_3 + \lambda \mu z_1z_2z_3$	\mathfrak{d}_{68} $1 + z_2z_3 + \mu z_1z_2z_3 + \lambda \mu z_1z_2^2z_3^2$	\mathfrak{d}_{6q} $1 + \lambda z_1z_2^2z_3$
\mathfrak{d}_{78} $1 + \lambda z_2 + \lambda z_2z_3$	\mathfrak{d}_{71} $1 + z_1 + z_3 + \mu z_1z_3$	\mathfrak{d}_{7q} $1 + \lambda z_2$
\mathfrak{d}_{81} $1 + z_2z_3 + \mu z_1z_2z_3$	\mathfrak{d}_{82} $1 + \lambda z_2 + \lambda z_2z_3 + \lambda z_2^2z_3$	\mathfrak{d}_{8q} $1 + \lambda \mu z_1z_2^2z_3$

The singular locus of N_U is given by the four rays $\mathbb{R}_{\geq 0}v_i$ for $i = 1, 3, 5, 7$, corresponding to the four non-toric boundary divisors of (X, D) .

4.3.3. A scattering diagram for U The finite cluster structure on U is equivalent to the existence of a consistent scattering diagram with a finite number of chambers. Consider the fan \mathcal{F} defined above. Let \mathfrak{d}_{ij} be the wall spanned by x_i and x_j , and let \mathfrak{d}_{iq} be the wall spanned by x_i and q_i . In what follows, when we refer to a wall \mathfrak{d}_{ij} it is convenient to implicitly allow $j = q$.

Proposition 4.12. *Decorating the walls of the fan \mathcal{F} with the wall functions given in Table 3 defines a consistent scattering diagram $\mathfrak{D}_{\lambda,\mu}$ in N_U .*

Proof. It is straightforward to check (via computer algebra) that composing the wall-crossing automorphisms corresponding to an oriented loop around any joint (i.e. a codimension 2 cone of \mathcal{F}) in $\mathfrak{D}_{\lambda,\mu}$ gives the identity. \square

Remark 4.13. The wall functions can be easily read off from the mutation relations. First note that, when expanded as a Laurent polynomial in x_1, q_1, x_3 , the cluster variables all have a monic leading monomial,⁹ i.e. the constant term of their numerator is equal to 1. Now the scattering function on the wall \mathfrak{d}_{ij} is obtained by substituting the leading monomial of each cluster variable (written in terms of z_1, z_2, z_3) into the righthand side of the corresponding mutation relation and clearing the denominators. For example crossing the wall \mathfrak{d}_{68} corresponds to the mutation $x_7q_2 = \lambda\mu + x_6 + \mu x_8 + x_6x_8$. If we substitute $x_6 \mapsto (z_1z_2z_3)^{-1}$ and $x_8 \mapsto (z_2z_3)^{-1}$ into the righthand side and clear the denominator we get the scattering function f_{68} in Table 3. Of course in general the scattering diagram is usually introduced in order to derive the mutation relations, not the other way round.

Since the mutation relations generating the cluster exchange graph for U are now easily read off as the wall-crossing automorphisms in $\mathfrak{D}_{\lambda,\mu}$, this shows that the cluster variables $x_1, \dots, x_8, q_1, q_2$ can now be recovered from $\mathfrak{D}_{\lambda,\mu}$ as the theta

⁹ This is not a happy accident. Indeed the rescaling that happens in Sect. 4.1.3 whilst deriving the equations of U was specially chosen in order to achieve this very fact.

functions attached to the integral points $v_1, \dots, v_8, v_{q_1}, v_{q_2} \in N_U(\mathbb{Z})$ respectively. Moreover, these could be computed by counting broken lines in $\mathfrak{D}_{\lambda, \mu}$.

Since the tropicalisation N_U also has the nice property that once a straight line has left a cone of \mathcal{F} it can never return, which can be seen by an explicit computation with affine structure of N_U as described in Lemma 4.11. Therefore, by a similar argument to the dimension 2 case Sect. 3.3.3, for all $a, b, c \geq 0$ the integral point $av_1 + bv_2 + cv_3 \in N_U(\mathbb{Z})$ belonging to the cone $\langle v_1, v_2, v_3 \rangle$ of \mathcal{F} must parameterise the theta function $\vartheta_{av_1+bv_2+cv_3} = \vartheta_{v_1}^a \vartheta_{v_2}^b \vartheta_{v_3}^c$, and similarly for all of the other cones of \mathcal{F} . This gives a complete description of the theta functions on U .

Relationship to the Argüz–Gross scattering diagram As described in Sect. 2.3.2, for any log Calabi–Yau variety with a suitably nice toric model Argüz and Gross [2] define a consistent scattering diagram by an inductive procedure, starting from an initial scattering diagram. Following this procedure in our case essentially recovers our special scattering diagram $\mathfrak{D}_{1,1}$.

Indeed, given the three centres $Z_1 = \mathbb{V}(x_1, 1 + q_1)$, $Z_2 = \mathbb{V}(q_1, 1 + x_1 + x_3 + \mu x_1 x_3)$ and $Z_3 = \mathbb{V}(x_3, 1 + \lambda q_1)$ in our toric variety X , their initial scattering diagram is built by attaching the nontrivial wall functions $1 + t_1 z_1$ to \mathfrak{d}_{71} , $1 + t_2 z_2$ to \mathfrak{d}_{1q} , \mathfrak{d}_{3q} , \mathfrak{d}_{5q} and \mathfrak{d}_{7q} , $1 + t_3 z_3$ to \mathfrak{d}_{35} and $(1 + t_1 z_1)(1 + t_3 z_3)$ to \mathfrak{d}_{13} . Here t_1, t_2 and t_3 are formal parameters (one for each centre Z_i) introduced to control the convergence of the wall functions in the case that the scattering diagram turns out not to be of finite type. The consistent scattering diagram obtained by their procedure should be the same as the one obtained from our diagram $\mathfrak{D}_{1,1}$ after substituting $z_i \mapsto t_i z_i$ for $i = 1, 2, 3$.

Enumerative interpretation of the walls Moreover, given our consistent scattering diagram $\mathfrak{D}_{1,1}$ it should now be possible to go one step further and understand the enumerative geometry of the log Calabi–Yau pair (\tilde{X}, \tilde{D}) in similar terms to the example studied in [2, 7]. Namely, for the wall functions $f_{\mathfrak{d}}$ appearing in the scattering diagram, one should be able to interpret the coefficients of the power series $\log f_{\mathfrak{d}}$ as punctured Gromov–Witten invariants for (\tilde{X}, \tilde{D}) . In particular, each of the eight interior divisors $E_{i,i+2} \subset U_{1,1}$ is isomorphic to $\mathbb{A}_{u,v}^2$, and hence each one contains a 2-dimensional family of \mathbb{A}^1 -curves $\{u^a = v^b : a, b \in \mathbb{Z}_{\geq 0}\}$ (i.e. smooth rational curves which, after further resolving (\tilde{X}, \tilde{D}) by toric blowups, intersect the boundary \tilde{D} transversely in one point). These should correspond to the eight wall functions of the form $1 + x + y + xy$ decorating $\mathfrak{d}_{i,i+2}$. The four interior divisors $F_{i,i+4} \subset U_{1,1}$ are all isomorphic to $\mathbb{A}^1 \times \mathbb{C}^\times$, and hence each one contains a unique deformation family of \mathbb{A}^1 -curves. These should correspond to the four wall functions of the form $1 + x$ decorating $\mathfrak{d}_{i,q} \cup \mathfrak{d}_{i+4,q}$. Lastly, the eight wall functions of the form $1 + x + y$ should correspond to the eight $\mathcal{O}(-1, -1)$ -curves in $\tilde{D} \subset \tilde{X}$ that are contracted to the eight (non-coordinate point) nodes $p \in D \subset X$ described in Lemma 4.1. Indeed, taking an appropriate affine neighbourhood of any one of these nodes gives the local SYZ singularity $X_{2,1}$ in the notation of [13], and the mirror $X_{1,2}$ has scattering diagram given by a single wall with a wall function of exactly this form.

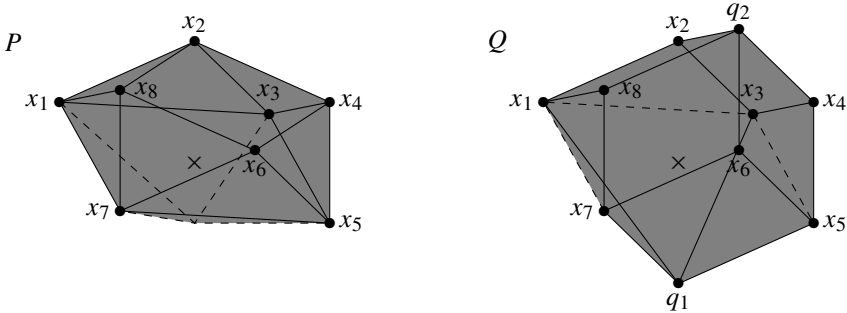
4.4. Applications to mirror symmetry

In this section, and until the end of the paper, we restrict to looking at the special fibre $U := U_{1,1}$ of our family \mathcal{U} of cluster varieties, corresponding to the values $\lambda = \mu = 1$. This is the most degenerate fibre, since it gains the two extra interior nodal singularities, and it is precisely the affine variety defined by the original recurrence relation (LR₃). The reason for this specialisation is that the expansions of the cluster variables as Laurent polynomials on a given cluster torus \mathbb{T}_{123} all now satisfy the binomial edge coefficient condition of Remark 2.14, which we expect for our mirror Landau–Ginzburg potentials. We continue to let (X, D) be the pair obtained by taking the projective closure $X = \overline{U} \subset \mathbb{P}^8$ with boundary divisor D .

4.4.1. Landau–Ginzburg models mirror to V_{12} and V_{16} We now describe how to construct explicit Landau–Ginzburg models which are mirror to the Fano 3-fold pairs considered in Sect. 1.2.2.

Proposition 4.14. *The polytopes $P = \text{conv}(x_1, \dots, x_8)$ and $Q = \text{conv}(x_1, \dots, x_8, q_1, q_2)$ are a pair of dual polytopes in M_U . Moreover they are, combinatorially, a realisation of the two polytopes of Fig. 8 when considered in the affine structure of M_U .*

Proof. When drawn with respect to the fan \mathcal{F} in \mathbb{R}^3 , the polytopes P and Q are pictured as follows



and so we are required to show that the dashed edges in the diagram are really flat when considered with respect to the affine structure on M_U .

The polytope P gives an integral piecewise-linear function $\phi_P : N_U \rightarrow \mathbb{R}$ given by $\phi_P(n) = \min\{c \in \mathbb{R} : n \in cP\}$, which is linear in each cone of our fan \mathcal{F} . Since $\phi_P(v_i) = 1$ for all $i \in \mathbb{Z}/8\mathbb{Z}$ and $\phi_P(w_1) = \phi_P(w_2) = 2$, this determines a Weil divisor $\Xi_P = D_1 + \dots + D_8 + 2D_{q_1} + 2D_{q_2}$ on \tilde{X} . Now any codimension 2 cone τ of \mathcal{F} , corresponds to a curve C_τ in the boundary of \tilde{X} . Using the criterion described in Sect. 2.3.1, the map ϕ_P is linear with respect to the affine structure on N_U if $\Xi_P \cdot C_\tau = 0$. Now we easily check that Ξ_P is only nonzero on the curve classes corresponding to the cones $\langle x_i, x_{i+1} \rangle$ and $\langle x_i, q_i \rangle$.

The computation is similar for the polytope Q , which corresponds to the Weil divisor $\Xi_Q = D_1 + \dots + D_8 + D_{q_1} + D_{q_2}$ on \tilde{X} . □

We now consider the two compactifications (X_P, D_P) and (X_Q, D_Q) of U which were discussed in Sect. 1.2.2. Note that $(X_P, D_P) = (X, D)$ is the standard projective compactification of U that we have been considering throughout this section.

An unprojection Before describing the mirror Landau–Ginzburg models to (X_P, D_P) and (X_Q, D_Q) , we explain how to go from one model to the other by making a birational modification $\psi : X_P \dashrightarrow X_Q$, called an *unprojection*. Geometrically, this contracts the two $\mathbb{P}^1 \times \mathbb{P}^1$ divisors $D_{1357}, D_{2468} \subset D$. This is done by adjoining $q_1 = x_0^{-1}(x_1x_5 - x_0^2)$ and $q_2 = x_0^{-1}(x_2x_6 - x_0^2)$, which are rational sections of $\mathcal{O}_X(1)$, as generators to the homogeneous coordinate ring $\mathbb{C}[X_P]$.

Proposition 4.15. *Let $X_Q =$*

$\{(x_0 : x_1 : \dots : x_8 : q_1 : q_2) \in \mathbb{P}^{10} : (x_0 : x_1 : \dots : x_8) \in X_P\}$ be the graph of the two rational sections q_1, q_2 on X_P . Then $X_Q \subset \mathbb{P}^{10}$ is a projectively Gorenstein 3-fold of codimension 7 determined by the 21 equations

$$x_i x_{i+3} = x_0(x_0 + x_{i+1} + x_{i+2}) \tag{\times 8}$$

$$x_i x_{i+4} = x_0(q_i + x_0) \tag{\times 4}$$

$$x_i q_{i+1} = (x_0 + x_{i+1})(x_0 + x_{i-1}) \tag{\times 8}$$

$$q_1 q_2 = x_0(4x_0 + x_1 + x_2 + x_3 + x_4 + x_5 + x_6 + x_7 + x_8) \tag{\times 1}$$

and has graded resolution with Betti numbers $(1, 21, 64, 70, 70, 64, 21, 1)$.

Proof. This is an application of the theory of unprojection developed by Papadakis–Reid [25]. The divisor $D_{q_1} = \mathbb{V}(x_0, x_2, x_4, x_6, x_8, x_1x_5 - x_3x_7) \subset \mathbb{P}^8$ is a complete intersection of codimension 6 (hence projectively Gorenstein) and contained in $X_P \subset \mathbb{P}^8$ which is projectively Gorenstein of codimension 5. By adjunction we have $K_{X_P} = \mathcal{O}_{X_P}(-1)$ and $K_{D_{q_1}} = \mathcal{O}_{D_{q_1}}(-2)$, and since $(-1) - (-2) = 1 > 0$ we can apply [25, Theorem 1.5] to obtain an unprojection variable q_1 as a rational section of $\mathcal{O}_{X_P}(1)$. We compute that $q_1 = x_0^{-1}(x_1x_5 - x_0^2)$ works as an unprojection variable, and satisfies the equations

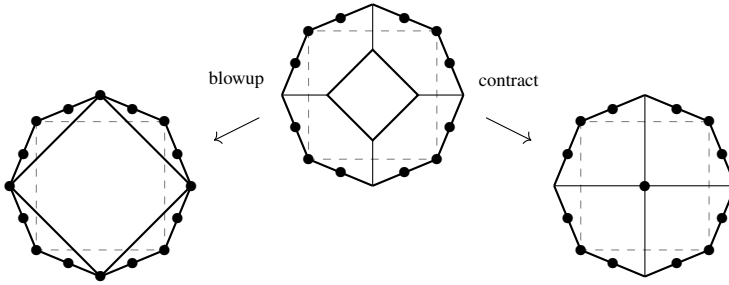
$$x_0 q_1 = x_1 x_5 - x_0^2 = x_3 x_7 - x_0^2,$$

$$x_i q_1 = (x_0 + x_{i-1})(x_0 + x_{i+1}) \quad \text{for } i = 2, 4, 6, 8$$

and thus we obtain an unprojection $(D_{q_1} \subset X_P) \dashrightarrow (P_{q_1} \in X'_P)$ which contracts D_{q_1} to an ordinary node at the coordinate point $P_{q_1} \in X'_P$. Now we repeat the procedure to the strict transform of D_{q_1} in X'_P to get $q_2 = x_0^{-1}(x_2x_6 - x_0^2)$ and an unprojection $(D_{q_2} \subset X'_P) \dashrightarrow (P_{q_2} \in X_Q)$. \square

Geometry of the unprojection The unprojection factors as a blowup of the (non-Cartier) Weil divisor D_{q_1} , which resolves four nodes of X_P , followed by the contraction of the strict transform to an ordinary node. The result of this operation is

depicted below. To construct X_Q we do this unprojection to both D_{q_1} and $D_{q_2} \subset X_P$ (i.e. to both the front and back squares of the diagram).



Note that the unprojection $\psi : X_P \dashrightarrow X_Q$ restricts to an isomorphism on the open set $U = X_P \setminus D_P$, since q_1 and q_2 are regular functions on U . Therefore if D_Q is the strict transform of the boundary divisor D_P then (X_Q, D_Q) is also a log Calabi–Yau compactification of U .

The potential w_Q According to Remark 2.14, since the ten nonzero integral points of Q are all vertices, the Landau–Ginzburg potential supported on Q that we consider is uniquely determined by summing the corresponding ten theta functions with coefficient 1, i.e.

$$w_Q = x_1 + x_2 + x_3 + x_4 + x_5 + x_6 + x_7 + x_8 + q_1 + q_2.$$

We note that this is σ_3 -invariant function and, indeed, restricting to the cluster torus chart $\mathbb{T}_{123} \subset U$ gives

$$(w_Q + 5)|_{\mathbb{T}_{123}} = \frac{(1 + x_1 + x_2)(1 + x_2 + x_3)(1 + x_1 + x_2 + x_3 + x_1x_3)}{x_1x_2x_3}$$

which is well-known to be an invariant function for Lyness map σ_3 .

The period $\pi_{w_Q}(t)$ Consider the period

$$\begin{aligned} \pi_{w_Q}(t) &= 1 + 48t^2 + 600t^3 + 13176t^4 + 276480t^5 + 6259800t^6 \\ &\quad + 146064240t^7 + \dots \end{aligned}$$

which agrees with the regularised quantum period $\widehat{G}_X(t)$ for the Fano 3-fold X of type V_{12} , as listed in [8, 13]. Alternatively, the shifted potential $w_Q + 5$ has period

$$\pi_{w_Q+5}(t) = 1 + 5t + 73t^2 + 1445t^3 + 33001t^4 + 819005t^5 + 21460825t^6 + \dots$$

which can be recognised as the Apéry series $\pi_{w+5}(t) = \sum_{n=0}^{\infty} \sum_{k=0}^n \binom{n}{k}^2 \binom{n+k}{k}^2 t^n$ and is also well-known as a mirror period sequence for the Fano 3-fold V_{12} , cf. [16].

A K3 fibration As we saw in the 2-dimensional examples of Sect. 3.4.2, smoothing a singular log Calabi–Yau pair (X, D) to a pair $(\widetilde{X}, \widetilde{D})$ consisting of a smooth Fano 3-fold \widetilde{X} with smooth anticanonical boundary divisor \widetilde{D} , corresponds under

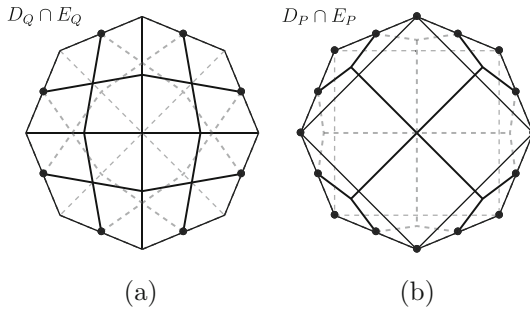


Fig. 12. **a** The sixteen lines of intersection for the boundary divisor D_Q and the degenerate interior divisor E_Q represented inside D_Q . **b** Similarly for the twelve lines of intersection of D_P and E_P

mirror symmetry to a compactification of the fibres of the mirror Landau–Ginzburg fibration. The Landau–Ginzburg model mirror to the smooth Fano 3-fold V_{2k} of Picard rank 1, is a fibration of K3 surfaces of Picard rank 19 (the fibration $\hat{\mathcal{X}}_k$ in the notation of [11]), and our self-mirror log Calabi–Yau 3-fold appears as an open subset in the fibration $\hat{\mathcal{X}}_6$, as we now describe.

In order to appreciate some beautiful geometry hiding here, it is convenient to consider extending the potential w_Q to the compactification X_Q . In analogy to the critical value -3 for the Landau–Ginzburg potential on the del Pezzo surface, the factorisation of $(w_Q + 5)|_{\mathbb{T}_{123}}$ corresponds to the fact that the interior divisor $E_Q := w_Q^{-1}(-5) \subset U$ is reducible. Then, in the notation of Proposition 4.7, the reducible fibre is $E_Q = \cup_{i=1}^8 E_{i,i+2}$ which is the union of eight copies of $\mathbb{P}^1 \times \mathbb{P}^1$ and happens to be isomorphic to D_Q (i.e. these eight components also meet like the faces of the polytope Q). The intersection of the divisors $D_Q \cap E_Q$ is a set of sixteen lines, given by the pair of lines on each face of D_Q which pass through the eight nodes $(1 : -1) \in \mathbb{P}^1_{x_i, x_{i+1}}$ in the boundary of X_Q . These lines are shown in Fig. 12.

Now the fibres of $w_Q: X_Q \dashrightarrow \mathbb{P}^1$ are given by the anticanonical pencil $|D_Q, E_Q|$ with baselocus the sixteen lines described above. The general such member of this pencil is a K3 surface $S_t := w_Q^{-1}(t)$ which is smooth, apart from eight ordinary double points which lie at the eight nodes of X that are contained in $D_Q \cap E_Q$. Therefore, after taking its minimal resolution, the K3 surface S_t contains a configuration $\Sigma = \cup_{i=1}^{24} \Sigma_i$ of 24 (-2) -curves with the dual intersection diagram displayed in Fig. 13a, where the black nodes correspond to the sixteen lines of $D_Q \cap E_Q$ and the white nodes correspond to the eight ordinary double points. Since the 24 (-2) -curves Σ span a lattice of rank 19 and S_t deforms in a nontrivial family, it follows that S_t has Picard rank 19.

Returning to our original Landau–Ginzburg model $w_Q: U \rightarrow C$, we see that the fibres are a family of affine K3 surfaces $w_Q^{-1}(t) = S_t \setminus \Sigma$, given by the complement of this configuration of lines Σ in S_t . These can be represented by as affine quartics

$$(t + 5)x_1x_2x_3 = (1 + x_1 + x_2)(1 + x_2 + x_3)(1 + x_1 + x_2 + x_3 + x_1x_3)$$

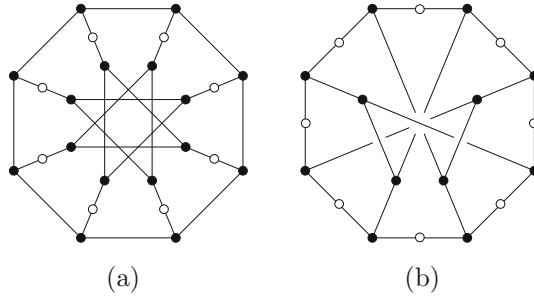
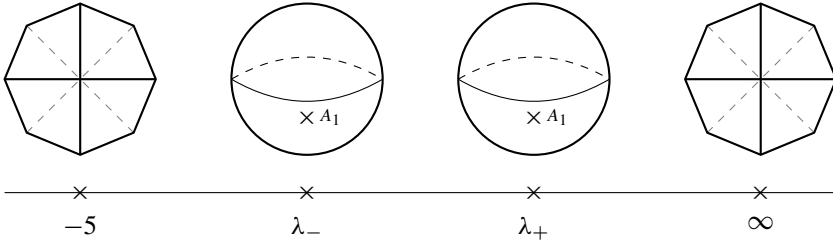


Fig. 13. **a** The configuration Σ of 24 (-2) -curves in the boundary of $w_Q^{-1}(t)$. **b** The configuration Σ of 20 (-2) -curves in the boundary of $w_P^{-1}(t)$

and there are precisely four degenerate fibres. Two reducible fibres corresponding to the values $E_Q = w_Q^{-1}(-5)$ and $D_Q = w_Q^{-1}(\infty)$, and two values $\lambda_{\pm} = 24(1 \pm \sqrt{2})$ which acquire an A_1 singularity. We get a picture as in the 2-dimensional case.



The potential w_P We can rerun this entire analysis with the potential $w_P = x_1 + \dots + x_8$ in place of w_Q . In summary, the period of w_P is

$$\pi_{w_P}(t) = 1 + 24t^2 + 192t^3 + 2904t^4 + 40320t^5 + 611520t^6 + 9515520t^7 + \dots$$

which agrees with the regularised quantum period $\widehat{G}_X(t)$ for the Fano 3-fold X of type V_{16} , as listed in [8, 15].

In this case the pencil of affine K3 surfaces determined by w_P specifies an open subset of the fibration $\widehat{\mathcal{X}}_7$ of [11], known to be mirror to the smooth Fano 3-fold V_{14} . There is a factorisation

$$(w_P + 4)|_{\mathbb{T}_{123}} = \frac{(1 + x_1)(1 + x_2)(1 + x_3)(1 + x_1 + x_2 + x_3)}{x_1x_2x_3}$$

which is another σ_3 -invariant Laurent polynomial, and corresponds to a reducible fibre given by $E_P := w_P^{-1}(-4) = \bigcup_{i=1}^4 F_{i,i+4}$ in the notation of Proposition 4.7. This reducible fibre E_P is the union of four rational surfaces intersecting like a tetrahedron in U . When extended to the compactification X_P , the boundary divisor D_P meets E_P in a collection of 12 lines, given by the Dih_8 -orbits of $\mathbb{V}(x_1 + x_2 + x_3) \subset D_{123}$ and $\mathbb{V}(x_1 + x_3) \subset D_{1357}$. These are displayed (tropically) in Fig. 12b and pass through the same eight nodes in the boundary of X_P as the previous case. The general member in the anticanonical pencil $|D_P, E_P|$, corresponding to the

fibres of w_Q , is a K3 surface $S_t = w_Q^{-1}(t)$ which passes through the twelve lines and is smooth apart from eight ordinary double points at the eight nodes of X_P . The minimal resolution of S_t is a K3 surface containing a configuration Σ of 20 (-2) -curves generating a lattice of Picard rank 19, and which correspond to the dual intersection diagram of Fig. 13b. The fibres of the original Landau–Ginzburg model $w_P: U \rightarrow \mathbb{C}$ are affine K3 surfaces of the form $S_t \setminus \Sigma$. There are exactly four degenerate fibres: the two reducible fibres $D_P = w_Q^{-1}(\infty)$ and $E_P = w_Q^{-1}(-4)$, and a further two values where the fibre obtains an A_1 singularity.

4.4.2. Other Fano 3-folds We do not try to attempt to classify all reflexive polytopes in N_U , although it would be interesting to know how many there are in comparison to the 4319 reflexive polytopes in \mathbb{R}^3 . Nevertheless, we can consider all of the polytopes obtained from removing vertices from the polytope Q from Sect. 4.4.1.

Theorem 4.16. *Consider the Laurent polynomial $w_0 = w|_{\mathbb{T}_{123}} \in \mathbb{C}[x_1^{\pm 1}, x_2^{\pm 1}, x_3^{\pm 1}]$ obtained by restricting the Landau–Ginzburg potential $w = \varepsilon_1 x_1 + \dots + \varepsilon_8 x_8 + \varepsilon_9 q_1 + \varepsilon_{10} q_2$ with coefficients $\varepsilon_i \in \{0, 1\}$ for $i = 1, \dots, 10$.*

1. *Of the 1024 possibilities for w_0 , 705 have 3-dimensional Fano Newton polytopes, i.e. $\text{Newt}(w_0)$ has primitive vertices and $0 \in \text{int}(\text{Newt}(w_0))$.*
2. *These 705 Laurent polynomials give rise to 46 distinct periods.*
3. *Of these 46 periods, 20 are equal to the regularised quantum period of a smooth Fano 3-fold, as described in Table 4.*

Table 4 only contains one representative Landau–Ginzburg potential in each case and, even after taking the Dih_8 symmetry into account, the same period sequence can be obtained from several different potentials. For example, in addition to the entry in the Table 4, the following five potentials also have the right period to be mirror to V_{22} :

$$x_1 + x_2 + x_5 + x_6 + q_2, \quad x_1 + x_2 + x_3 + x_4 + x_5 + q_2, \quad x_1 + x_2 + q_1 + q_2, \\ x_1 + x_2 + x_3 + x_4 + x_5 + x_7 \quad \text{and} \quad x_1 + x_2 + x_3 + x_4 + x_6 + q_2.$$

According to Conjecture 2.13, the different choices of potential correspond to different degenerations of a Fano 3-fold of type V_{22} to a pair (X_Q, D_Q) where Q is the dual polytope to $P = \text{Newt}(w) \subset M_U$. It would be interesting to know whether the remaining 26 period sequences are all period sequences of Fano 3-folds with terminal singularities.

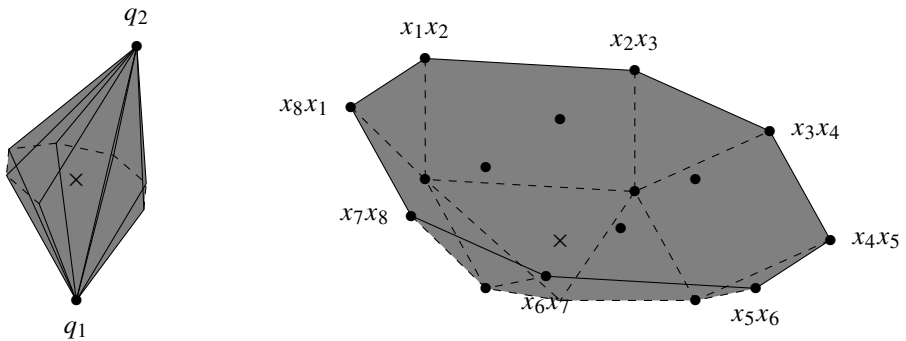
4.4.3. A final example We end with a final example of mirror duality for a pair of exotic polytopes in N_U , which cannot be realised combinatorially as polytopes in Euclidean space. The intersection of the two halfspaces $(q_1)^{\geq -1} \cap (q_2)^{\geq -1}$ is a closed polytope $Q \subset N_U$ with eight vertices $x_i x_{i+1}$ for $i \in \mathbb{Z}/8\mathbb{Z}$. Therefore the dual polytope P is given by $P = \bigcap_{i \in \mathbb{Z}/8\mathbb{Z}} (x_i x_{i+1})^{\geq -1}$. This gives a pair of dual polytopes in N_U

$$P = \text{conv}(q_1, q_2) \quad \text{and} \quad Q = P^* = \text{conv}(x_1 x_2, x_2 x_3, \dots, x_8 x_1).$$

Table 4. Mirror Landau–Ginzburg potentials on U for 20 smooth Fano 3-folds

Fano 3-fold	Mirror Landau–Ginzburg potential w
V_{12}	$x_1 + x_2 + x_3 + x_4 + x_5 + x_6 + x_7 + x_8 + q_1 + q_2$
V_{14}	$x_1 + x_2 + x_3 + x_4 + x_5 + x_6 + x_7 + x_8 + q_1$
V_{16}	$x_1 + x_2 + x_3 + x_4 + x_5 + x_6 + x_7 + x_8$
V_{18}	$x_1 + x_2 + x_3 + x_4 + x_5 + x_6 + x_7$
V_{22}	$x_1 + x_2 + x_3 + x_4 + x_5 + x_6$
$MM_{2,9}$	$x_1 + x_2 + x_3 + x_6 + q_1 + q_2$
$MM_{2,12}$	$x_1 + x_2 + x_3 + x_5 + x_6 + x_7$
$MM_{2,13}$	$x_1 + x_2 + x_3 + x_4 + x_6 + x_7$
$MM_{2,14}$	$x_1 + x_2 + x_3 + x_4 + x_5 + x_7 + q_1$
$MM_{2,16}$	$x_1 + x_2 + x_3 + x_6 + q_1$
$MM_{2,17}$	$x_1 + x_2 + x_3 + x_5 + x_6$
$MM_{2,20}$	$x_1 + x_2 + x_3 + x_4 + x_7$
$MM_{2,21}$	$x_1 + x_2 + x_3 + x_5 + x_7$
$MM_{2,22}$	$x_1 + x_2 + x_3 + x_6$
$MM_{3,7}$	$x_1 + x_2 + x_4 + x_6 + x_7$
$MM_{3,10}$	$x_1 + x_2 + x_3 + x_5 + x_7 + q_1$
$MM_{3,12}$	$x_1 + x_3 + x_6 + x_7 + q_1$
$MM_{3,13}$	$x_1 + x_5 + q_2$
$MM_{3,15}$	$x_1 + x_4 + x_5 + x_7$
$MM_{3,20}$	$x_1 + x_4 + x_6$

We draw these two polytopes below, where the solid lines denote edges of the polytope and dashed lines are due to the bend in the affine structure of N_U . We note that P has two vertices and eight faces (so topologically it looks like a beachball with eight stripes), whereas Q has eight vertices and two faces.



We now describe how to set up the mirror correspondence between the (degenerate) Fano 3-fold (X_P, D_P) (resp. (X_Q, D_Q)) and the Landau–Ginzburg model (U, w_Q) (resp. (U, w_P)).

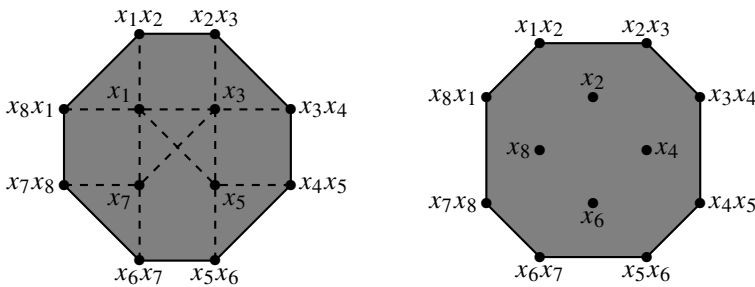
Example 4.17. We start by describing the mirror correspondence for (X_Q, D_Q) and (U, w_P) .

The Landau–Ginzburg model (U, w_P) Using P as the polytope to define a Landau–Ginzburg model (U, w_P) is straightforward, since P contains only two nonzero lattice points which are both vertices. By Remark 2.14 they both receive coefficient 1 and this uniquely determines the potential $w_P = q_1 + q_2$. By restricting to the torus chart \mathbb{T}_{123} and computing the period sequence of the resulting Laurent polynomial, we find that

$$\pi_{w_P}(t) = 1 + 8t^2 + 24t^3 + 240t^4 + 1440t^5 + 11960t^6 + 89040t^7 + \dots$$

which is the regularised quantum period of the smooth Fano 3-fold $\text{MM}_{2,21}$ [8, 38].

The Fano 3-fold (X_Q, D_Q) When considered in the integral affine structure of M_U , the two faces of Q are two flat lattice octagons labelled with the following theta functions.



Thus to construct (X_Q, D_Q) we consider the graded ring R_Q which is generated in degree 1 by seventeen generators

$$x_0, x_1, \dots, x_8, x_1x_2, \dots, x_8x_1$$

where x_0 is the homogenising variable. According to computer algebra $X_Q = \text{Proj } R_Q \subset \mathbb{P}^{16}$ is a Gorenstein Fano variety of Fano index 1 and degree $\text{deg } X_Q = \text{vol } Q = 28$. This at least agrees with X_Q being a (degeneration of a) Fano 3-fold of type $\text{MM}_{2,21}$, as predicted by the period sequence of w_P . By Conjecture 2.13 we expect that X_Q admits a \mathbb{Q} -Gorenstein smoothing to a smooth Fano 3-fold of type $\text{MM}_{2,21}$.

Moreover, the boundary divisor $D_Q = \mathbb{V}(x_0)$ consists of two components $D = D_1 \cup D_2$ which are toric surfaces (defined by the two octagons above) which glued together other along an octagon of rational curves. This realises Q as the intersection complex of D_Q .

Example 4.18. The more interesting (and currently less clear) direction is to understand how to set up the mirror correspondence with the roles of P and Q reversed. It suggests the possibility of constructing at least three different deformation families of Fano 3-folds with the Hilbert series [6, #14885] in the Graded Ring database. Currently two such families are known: one constructed as a complete intersection in a toric variety [19] and the other via unprojection [26] (although it is not known whether these two families are distinct).

The Fano 3-fold (X_P, D_P) The polytope P gives degrees $2, 2, \dots, 2, 1, 1$ to the variables $x_1, x_2, \dots, x_8, q_1, q_2$ respectively. Taking the projective closure of U with respect to this grading we get a Fano 3-fold $X_P = \text{Proj } R_P \subset \mathbb{P}(1^3, 2^8)$ in weighted projective space. One of the equations defining X_P is

$$q_1q_2 = x_1 + x_2 + x_3 + x_4 + x_5 + x_6 + x_7 + x_8 + 4x_0^2$$

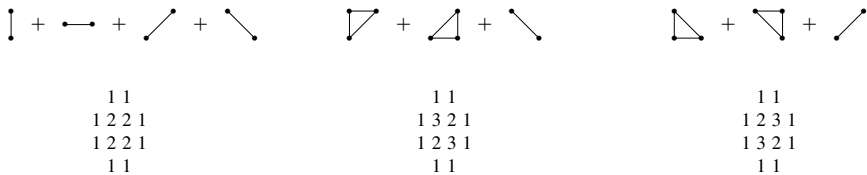
which we could use to eliminate x_1 say, and reduce to a model $X_P \subset \mathbb{P}(1^3, 2^7)$. The Hilbert series of X_P now agrees with [6, #14885], showing that X_P has degree $\text{deg}(X_P) = \text{vol}(P) = 4$, Fano index 1 and basket of quotient singularities $\{8 \times \frac{1}{2}(1, 1, 1)\}$. The anticanonical boundary divisor $D_P = \mathbb{V}(x_0)$ has eight components:

$$D_{12} = \mathbb{V}(x_0, x_3, x_4, x_5, x_6, x_7, x_8, q_1q_2 - x_1 - x_2) \text{ etc.}$$

which are all copies of $\mathbb{P}(1, 1, 2)$ that are joined to their neighbours along conics meeting at the two coordinate points where $q_1 \neq 0$ and $q_2 \neq 0$. Thus P is realised as the intersection complex for the boundary divisor D_P . One of the eight $\frac{1}{2}(1, 1, 1)$ points of X_P lies in the relative interior of D_{12} at the point where $x_1 + x_2 \neq 0$ and all of the other coordinates vanish. Similarly for the other seven $\frac{1}{2}(1, 1, 1)$ points.

We note that if Y is a Fano 3-fold with Hilbert series [6, #14885], then $h^0(Y, -K_Y) = 3$ and hence $-K_Y$ is ample but not very ample, so there is no Gorenstein toric degeneration of Y . Therefore there is no reflexive polytope we can write down which will give us a mirror Laurent polynomial for Y .

The Landau–Ginzburg model (U, w_Q) To cook up a Landau–Ginzburg potential w_Q which is mirror to (X_P, D_P) , we need to label the lattice points of Q with appropriate integer coefficients, as described in Remark 2.14. Since we label all vertices of Q with the coefficient 1, the only decisions we need to make are over the lattice points belonging to the relative interior of each face. Following [10], we expect that the right thing to do is label the lattice points of each face $F \subset Q$ with the coefficients of a *0-mutable polynomial* supported on F . In our case this is one of the following three choices of coefficients, according to the three possible maximal Minkowski decompositions of the octagon.



After taking into account the Dih_8 symmetry, there are just three ways to decorate Q with coefficients, yielding three Landau–Ginzburg potentials with distinct periods. As described in Remark 2.14, according to Conjecture 2.13 these are conjecturally in one-to-one correspondence with three possible deformations of X_P . None of these three periods appear in the classification of quantum periods for smooth Fano 3-folds [8], which is unsurprising since X_P has isolated terminal quotient singularities (which cannot be deformed away by any smoothing). However it suggests

that X_P may lie at the intersection of three different components of Fano 3-folds in its Hilbert scheme.

Remark 4.19. Smoothings of Gorenstein *toric* Fano 3-folds (X_P, D_P) associated to an (honest) reflexive polytope $P \subset \mathbb{R}^3$ have been studied in [9], and their construction requires the input of a Minkowski decomposition of each facet of P . Different choices of Minkowski decompositions lead to topologically distinct smoothings.

Acknowledgements I would like to thank Alessio Corti, Alastair King, Andy Hone and Thomas Prince, amongst a number of others, for helpful discussions on the subject of this paper. In particular, Alessio Corti first proposed the geometric definition of a seed described in Sect. 2.2.2, Alastair King suggested formulating the material in Sect. 4.1 using the spin representation of B_4 (rather than the half-spin representation of D_5) and Thomas Prince helped derive the scattering diagram described in Sect. 4.3.3. Moreover, I thank the anonymous referee for a number of suggestions which have greatly improved this paper, and, in particular, in Sect. 4.1.4 a formulation for the construction of our main family in the terms of the Gross–Siebert program.

Data availability Data sharing is not applicable to this article as no datasets were generated or analysed during the current study.

Open Access This article is licensed under a Creative Commons Attribution 4.0 International License, which permits use, sharing, adaptation, distribution and reproduction in any medium or format, as long as you give appropriate credit to the original author(s) and the source, provide a link to the Creative Commons licence, and indicate if changes were made. The images or other third party material in this article are included in the article's Creative Commons licence, unless indicated otherwise in a credit line to the material. If material is not included in the article's Creative Commons licence and your intended use is not permitted by statutory regulation or exceeds the permitted use, you will need to obtain permission directly from the copyright holder. To view a copy of this licence, visit <http://creativecommons.org/licenses/by/4.0/>.

Declarations

Conflict of interest The author states that there are no conflicts of interest.

References

- [1] Akhtar, M., Coates, T., Corti, A., Heuberger, L., Kasprzyk, A., Oneto, A., Petracci, A., Prince, T., Tveiten, K.: Mirror symmetry and the classification of orbifold del Pezzo surfaces. *Proc. Am. Math. Soc.* **144**, 513–527 (2016)
- [2] Argüz, H., Gross, M.: The higher dimensional tropical vertex. [arXiv:2007.08347](https://arxiv.org/abs/2007.08347)
- [3] Auroux, D., Katzarkov, L., Orlov, D.: Mirror symmetry for del Pezzo surfaces: vanishing cycles and coherent sheaves. *Inventiones mathematicae* **166**, 537–582 (2006)
- [4] Beauville, A.: Les familles stables de courbes elliptiques sur \mathbb{P}^1 admettant quatre fibres singulières. *C. R. Acad. Sci. Paris* **294**, 657–660 (1982)
- [5] Beukers, F.: Irrationality of π^2 , periods of an elliptic curve and $\Gamma_1(5)$. In: Bertrand, D., Waldschmidt, M. (eds.) *Proceedings “Approximations diophantiennes...”*, Luminy 1982, *Progress in Mathematics*. Birkhäuser (1983)

- [6] Brown, G., Kasprzyk, A., et al.: The graded ring database. www.grdb.co.uk
- [7] Coates, T., Corti, A., Galkin, S., Golyshev, V., Kasprzyk, A.: Mirror symmetry and Fano manifolds. In: European Congress of Mathematics (Kraków, 2-7 July), pp. 285–300 (2013)
- [8] Coates, T., Corti, A., Galkin, S., Kasprzyk, A.: Quantum periods for 3-dimensional Fano manifolds. *Geom. Topol.* **20**(1), 103–256 (2016)
- [9] Coates, T., Corti, A., da Silva Jr, G.: On the topology of Fano smoothings. [arXiv:1912.04383](https://arxiv.org/abs/1912.04383)
- [10] Corti, A., Filip, M., Petracci, A.: Mirror symmetry and smoothing Gorenstein toric affine 3-folds. [arXiv:2006.16885](https://arxiv.org/abs/2006.16885)
- [11] Doran, C., Harder, A., Novoseltsev, A., Thompson, A.: Calabi–Yau threefolds fibred by high rank lattice polarized K3 surfaces. *Mathematische Zeitschrift* **294**, 783–815 (2020)
- [12] Gross, M., Hacking, P., Keel, S.: Mirror symmetry for log Calabi–Yau surfaces I. *Publ. Math. Inst. Hautes Études Sci.* **122**(1), 65–168 (2015)
- [13] Gammage, B.: Local mirror symmetry via SYZ. [arXiv:2105.12863](https://arxiv.org/abs/2105.12863)
- [14] Gross, M., Hacking, P., Keel, S.: Birational geometry of cluster algebras. *Algebraic Geom.* **2**(2), 137–175 (2015)
- [15] Gross, M., Siebert, B.: Intrinsic mirror symmetry and punctured Gromov–Witten invariants, algebraic geometry: Salt Lake City 2015. *Proc. Sympos. Pure Math.* **97**(2), 199–230 (2018)
- [16] Golyshev, V., Zagier, D.: A proof of the Gamma Conjecture for Fano 3-folds of Picard rank 1. *Izvestiya: Math.* **80**(1), 27–54 (2016)
- [17] Hacking, P., Keel, S.: Mirror symmetry and cluster algebras. *Proc. Int. Cong. Math. (Rio de Janeiro)* **2**, 689–716 (2018)
- [18] Hacking, P., Keel, S., Yu, T.Y.: Secondary fan, theta functions and moduli of Calabi–Yau pairs. [arXiv:2008.02299](https://arxiv.org/abs/2008.02299)
- [19] Hausen, J., Mauz, C., Wrobel, M.: The Anticanonical complex for non-degenerate toric complete intersections. *Manuscripta Math.* (2022)
- [20] Katzarkov, L., Kontsevich, M., Pantev, T.: Bogomolov–Tian–Todorov theorems for Landau–Ginzburg models. *J. Differ. Geom.* **105**(1), 55–117 (2017)
- [21] Kollár, J.: Sources of log canonical centers, in Minimal models and extremal rays, Kyoto 2011. *Adv. Stud. Pure Math.* **70**, 29–48 (2016)
- [22] Lai, J., Zhou, Y.: Mirror Symmetry for log Calabi–Yau Surfaces II. [arXiv:2201.12703](https://arxiv.org/abs/2201.12703)
- [23] Lam, T., Pylyavskyy, P.: Laurent phenomenon algebras. *Camb. J. Math.* **4**, 121–162 (2016)
- [24] Mandel, T.: Tropical theta functions and log Calabi–Yau surfaces. *Sel. Math. New Ser.* **22**, 1289–1335 (2016)
- [25] Papadakis, S., Reid, M.: Kustin–Miller unprojection without complexes. *J. Algebraic Geom.* **13**, 563–577 (2004)
- [26] Petrotou, V.: Tom and Jerry triples with an application to Fano 3-folds. *Commun. Algebra* **50**(9), 3960–3977 (2022)